



## Beachrock-type calcarenitic tsunamites along the shores of the eastern Ionian Sea (western Greece) – case studies from Akarnania, the Ionian Islands and the western Peloponnese

Andreas Vött, Georg Bareth, Helmut Brückner, Constanze Curdt, Ioannis Fountoulis, Ralf Grapmayer, Hanna Hadler, Dirk Hoffmeister, Nicole Klasen, Franziska Lang, Peter Masberg, Simon Matthias May, Konstantin Ntageretzis, Dimitris Sakellariou and Timo Willershäuser

with 18 figures and 2 tables

**Summary.** This paper presents geo-scientific evidence of beachrock-type calcarenitic tsunamites from three study areas in western Greece, namely from the Bays of Aghios Nikolaos (Akarnania), Langadakia (Cefalonia Island) and Aghios Andreas (Peloponnese). Geomorphological, sedimentological, micromorphological and geochemical studies were conducted to clarify depositional processes and the post-sedimentary evolution. Calcarenitic and locally conglomeratic carbonate crusts were studied in natural outcrops along the seafront and in vibracores. High-resolution topographic surveys and 3D-visualisation were carried out by differential GPS and LIDAR measurements. Tsunami impact was dated by a combined approach of radiocarbon, OSL and archaeological age determination and compared to local tsunami and earthquake chronologies.

We found sedimentary structures such as basal unconformities, rip-up and intra-clasts, evidence of fining upward, thinning landward and upward increase in sorting as well as bi-to multimodal deposits and injection structures all of which are described as features typical of recent or historic tsunami deposits. Typically non-littoral sedimentary features such as load casts and convolute bedding further indicate gravity driven processes in water-saturated sheets of allochthonous deposits and are well known from, for example, turbidites. Moreover, thin section analyses revealed high-energy shock- and impact-borne cracking and shearing effects. Our results show that cementation of tsunami deposits may occur by post-depositional pedogenetic decalcification of higher sections and subsequent secondary carbonate precipitation in lower sections of tsunami deposits provided that they were deposited above sea level. The calcarenitic tsunamites encountered in the three study areas match the definition of beachrock *sensu stricto*. This is thus the first paper giving examples of beachrock sequences that are interpreted as partially cemented tsunami deposits. Consequently, beachrock is recommended not to be used as sea level indicator in future studies unless a tsunami-genic formation can be definitely excluded.

Dating results brought to light young, mostly Holocene ages of tsunami sediments. In the Bay of Aghios Andreas, western Peloponnese, we found spectacular traces that Olympia's ancient harbour site Pheia was destroyed by tsunami impact in the 6<sup>th</sup> cent. AD and covered by a rapidly cemented, up to 3 m-thick beachrock-type tsunami deposit.

**Zusammenfassung.** Dieser Aufsatz stellt geowissenschaftliche Belege für Beachrock-artige kalkarenitische Tsunamite aus drei Untersuchungsgebieten Westgriechenlands vor, nämlich der Bucht von Aghios Nikolaos (Akarnanien), der Bucht von Langadakia (Kephallonia) und der Bucht von Aghios Andreas (Peloponnes). Geomorphologische, sedimentologische, mikromorphologische und geochemische Analysen dienten der Klärung von Ablagerungsprozessen und der postsedimentären Entwicklung. Kalkarenitische und lokal konglomeratische Karbonatkrusten wurden in natürlichen

Aufschlüssen entlang der Wasserlinie und in Schlaghammerbohrungen untersucht. Hochauflösende topographische Vermessungen und 3D-Visualisierungen wurden mit Hilfe von Differenzial-GPS und LIDAR durchgeführt. Tsunami-Ereignisse wurden mittels eines kombinierten Ansatzes aus Radiokohlenstoff-Analysen, OSL-Messungen und archäologischen Altersbestimmungen datiert und mit lokalen Tsunami- und Erdbebenchronologien verglichen.

Vorgefundene sedimentäre Strukturen wie basale Erosionsdiskordanzen, rip-up und intra-clasts, Belege für fining upward- und thinning landward-Sequenzen und eine nach oben gerichtete Zunahme des Sortierungsgrades sowie bi- bis multimodale Ablagerungen und Injektionsstrukturen entsprechen Charakteristika sowohl rezenter als auch historischer Tsunamis. Desweiteren belegen Belastungsmarken (load casts) und Wickelschichtung (convolute bedding) Schwerkraft-induzierte Verlagerungsprozesse in wassergesättigten Sequenzen allochthoner Ablagerungen, die in gewöhnlichen litoralen Systemen nicht vorkommen, aber beispielsweise von Turbiditen bekannt sind. Die Analyse von Dünnschliffen ergab außerdem Spuren hochenergetischer, schock- und impaktbürtiger Aufspaltungen und Zerscherungen im Mikrobereich. Unsere Untersuchungen belegen weiterhin, dass die Zementierung von Tsunami-Ablagerungen durch postsedimentäre pedogentische Entkalkung in höheren und sekundäre Karbonatausfällung in tieferen Schichten von Tsunami-Ablagerungen stattfinden kann, sofern diese Sedimente oberhalb des Meeresspiegel abgelagert wurden.

Die in den drei Untersuchungsgebieten vorgefundenen kalkarenitischen Tsunamite entsprechen der Definition von Beachrock *sensu stricto*. Der vorliegende Aufsatz liefert daher erstmalig Beispiele für Beachrock-Sequenzen, die partiell zementierte Tsunami-Ablagerungen darstellen. Es wird daher empfohlen, von der Verwendung von Beachrock als Meeresspiegelindikator in zukünftigen Untersuchungen abzusehen, sofern eine tsunamigene Bildung des Vorkommens nicht ausgeschlossen werden kann.

Die im Rahmen der Studie durchgeführten Datierungen erbrachten junge, meist holozäne Alter der Tsunami-Ablagerungen. In der Bucht von Aghios Andreas, westliche Peloponnes, konnten spektakuläre Belege für eine Zerstörung des antiken Hafens von Olympia im 6. Jahrhundert nach Christus und dessen Überdeckung durch rasch zementierte, bis zu 3 m mächtige Beachrock-artige Tsunami-Ablagerungen gefunden werden.

## 1 Introduction

Tsunami hazard in the eastern Mediterranean belongs to the highest worldwide. This is mostly due to the high seismic activity along the Hellenic Arc where the African Plate is being subducted under the Eurasian Plate inducing numerous strong tsunamigenic earthquakes. Also, the Arabian Plate, moving northward by high rates, is a serious source of seismically related hazards. Further potential tsunami triggers in the Mediterranean are submarine slides, meteorite impacts, and explosional volcanic activity, for instance around Sicily or in the Aegean Sea. The eastern Mediterranean is characterized by comparatively short shore-to-shore distances, a highly variable underwater topography and thousands of kilometers of coastline with numerous indentations. In terms of tsunami hazard, this constellation implicates short time intervals for advance warning of local populations, strong refraction effects difficult to predict and a variety of secondary, mostly earthquake-related hazards such as rockfall, liquefaction and subaerial and underwater landslides.

Palaeotsunami research in the eastern Mediterranean has been strongly intensified during the past decades in order to improve our understanding of the dimension and the dynamic of tsunami landfalls and to gain reliable background information for future risk

assessment (e.g. SHAW et al. 2008). Besides archival studies based on ancient accounts and historical data related to extreme wave events in the Mediterranean (GUIDOBONI et al. 1994, SOLOVIEV et al. 2000, PAPADOPOULOS 2001, TINTI et al. 2004, GUIDOBONI & COMASTRI 2005, PAPADOPOULOS & FOKAEFS 2005, PAPADOPOULOS et al. 2007, SCHIELEIN et al. 2007, NGDC 2009), an increasing number of geo-scientific field studies have been carried out to detect palaeotsunami deposits. These tsunami deposits can be classified into three main groups. The first group comprises dislocated boulders, originating from bedrock units within the littoral zone, that were torn out, uplifted, turned over and/or transported dozens of meters inland by tsunamigenic wave action. Such deposits are reported from southern Italy (e.g. MASTRONUZZI & SANSÒ 2000, 2004, MASTRONUZZI et al. 2007, SCICCHITANO et al. 2007, PANTOSTI et al. 2008), the Ionian Islands, the Peloponnese, and Crete (e.g. SCHEFFERS & SCHEFFERS 2007, SCHEFFERS et al. 2008, VÖTT et al. 2009a), southern Turkey (KELLETTAT 2005), Cyprus (KELLETTAT & SCHELLMANN 2002) and from the Levantine coast (MORHANGE et al. 2006a, see also MORHANGE et al. 2006b). In the western Mediterranean, tsunamigenically dislocated boulders were recently described from the Algerian and Tunisian coasts (MAOUCHE et al. 2009, MAY et al. 2009). The second group is represented by allochthonous marine sediments, mostly sand and/or gravel, found in sub- and supra-littoral or near-shore geological archives and sometimes associated to cultural debris. Examples are known from Italy (GIANFREDA et al. 2001, DE MARTINI et al. 2003), mainland Greece (PIRAZZOLI et al. 1999, DOMINEY-HOWES et al. 2000, GAKI-PAPANASTASSIOU et al. 2001, KORTEKAAS 2002, VÖTT et al. 2007, 2008), the Aegean Islands (MCCOY & HEIKEN 2000, BRUINS et al. 2008), Israel (REINHARDT et al. 2006) and from Egypt (BERNASCONI et al. 2006, STANLEY & BERNASCONI 2006). The third group comprehends allochthonous fine-grained tsunami deposits intersecting homogeneous autochthonous sediments of near-shore swamps, quiescent freshwater lakes or lagoonal environments. Studies from Akarnania, the Ionian Islands (VÖTT et al. 2009a, 2009b) and the Peloponnese (KONTOPOULOS & AVRAMIDIS 2003) show that this group offers the best premises for sandwich radiocarbon dating of event deposits. This is due to weaker erosional dynamics and the large availability of datable in-situ organic material not affected by marine reservoir effects.

This paper presents a fourth group of tsunami deposits, so far unknown, based on three case studies on beachrock-type calcarenitic tsunamites from western Greece. In this area, previous investigations have revealed multiple tsunami impact since the mid-Holocene (VÖTT et al. 2006, 2007, 2008, 2009a, 2009b, MAY et al. 2007). The main objectives of our studies were (i) to describe the sedimentary and micromorphological characteristics of the calcarenites, (ii) to clarify, where possible, how their cementation took place, (iii) to comprehend the dynamic processes of sedimentation by a combined approach of geomorphological, sedimentological and geoarchaeological methods, and (iv) to apply radiocarbon and OSL dating techniques and geoarchaeological age determination in order to compare the results with existing local geochronostratigraphies. Research was conducted within the framework of an interdisciplinary project on tsunami traces along the shores of the eastern Ionian Sea opposite to the Hellenic Arc.

## 2 Topographic and geotectonic settings

The study sites presented in this paper are (i) the Bay of Aghios Nikolaos in northwestern Akarnania, (ii) the Bay of Langadakia on the western coast of the Paliki Peninsula, Cefalonia Island, and (iii) the Bay of Aghios Andreas on the western side of the Katakolo Promontory in the western Peloponnese (Fig. 1). All three areas are directly exposed to the western

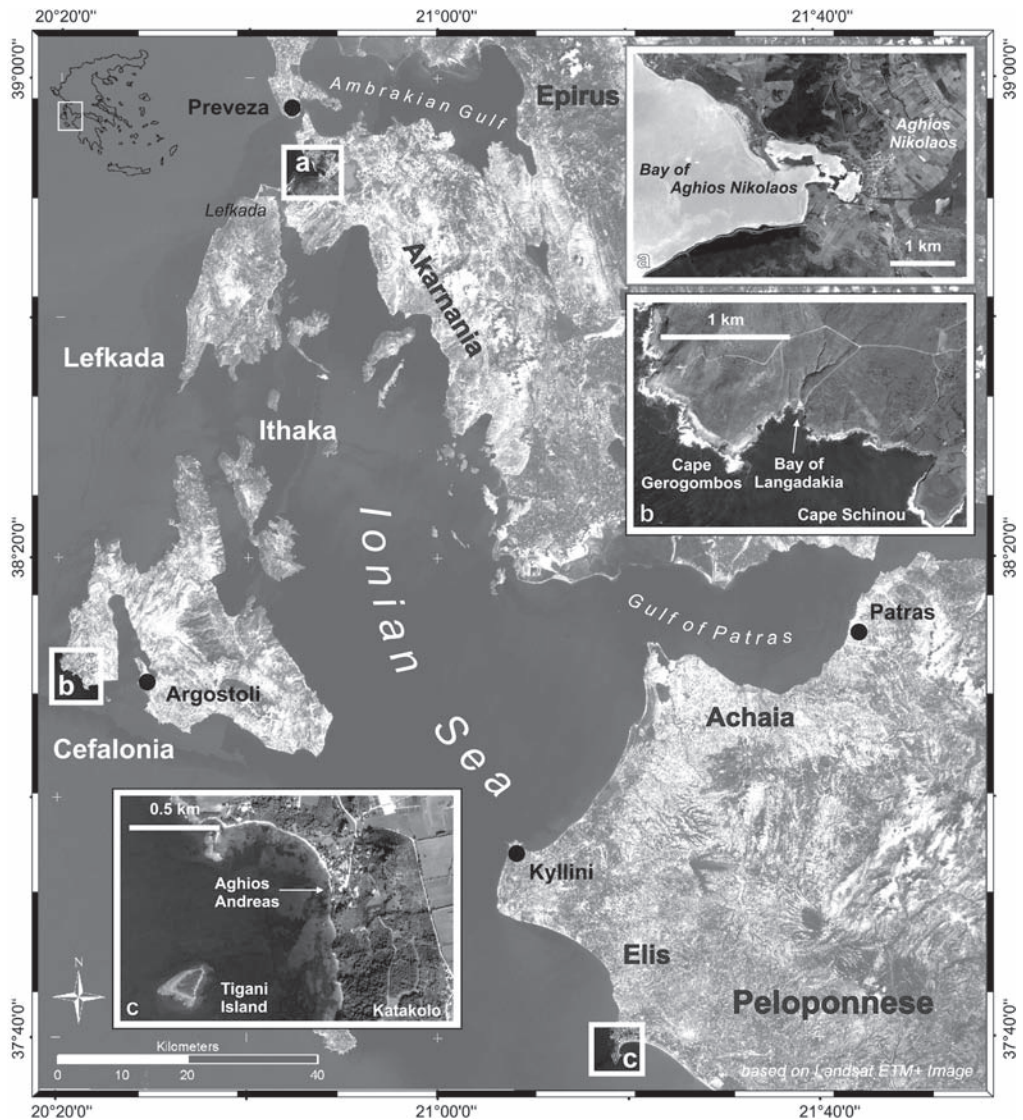


Fig. 1. Topographic overview of western Greece and the study sites presented in this paper, all of them located along the shores of the eastern Ionian Sea. (a) Bay of Aghios Nikolaos, Akarnania; (b) Bay of Langadakia, Cefalonia Island; (c) Bay of Aghios Andreas, Peloponnese. General map based on Landsat ETM+ (2000), inlay maps based on Google Earth images (2003–2005).

section of the Hellenic Arc. Concerning bathymetrical conditions, water depths reach 4 to 5 km in the Hellenic Trench and the adjacent abyssal plains (HIEKE et al. 2003) only 50 to 250 km offshore the Peloponnese. The shelf zone around the Bay of Aghios Nikolaos is comparatively wide whereas it narrows considerably towards the western coasts of Cefalonia Island and the western Peloponnese.

The Hellenic Arc represents a zone of different types of plate boundaries with predominant subduction of the African Plate beneath the Aegean microplate, the latter being driven into a southwestward direction (SACHPAZI et al. 2000) by the Arabian and Anatolian Plates that are rapidly moving northward and westward, respectively. The right-lateral strike slip Cefalonia transform fault (CF) marks the transition from subduction to collision in the northwestern arc zone. Rates of crustal motion to the north and west of the CF remain below 5 mm/a but strongly increase towards the SE reaching up to 30 mm/a in the southern Peloponnese and 40 mm/a in Crete (KAHLE et al. 1993, 1995, COCARD et al. 1999, McCLUSKY et al. 2000). Since Oligo-Miocene times, this rapid southwestward movement of the Aegean Plate has caused pull-apart dynamics in western mainland Greece (PAPAZACHOS & KIRATZI 1996, DOUTSOS & KOKKALAS 2001) in combination with considerable clockwise rotations of larger crustal units such as the Akarnanian block (BROADLEY et al. 2004, VAN HINSBERGEN et al. 2005). As revealed by continuous GPS studies, the same process also induced crustal compression between the Ionian Islands and the Greek mainland (HOLLENSTEIN et al. 2008a). The western Hellenic Arc belongs to the seismically most active regions all over Europe (PAPAZACHOS & PAPAZACHOU 1997) and is responsible for a high tsunami risk (PAPAZACHOS & DIMITRIU 1991) which is also shown by local to regional earthquake and tsunami catalogues (PAPADOPOULOS 2001, PAPADOPOULOS & FOKAEFS 2005, see also VÖTT et al. 2006).

The surrounding of the Bay of Aghios Nikolaos is characterized by locally brecciated Triassic to early Tertiary dolomite and limestone (IGME 1996), that of the Bay of Langadakia by thick units of Eocene limestone (IGME 1985). In both cases, bedrock is fairly resistant to subaerial weathering and coastal erosion; local fault systems trend prevalently in SW-NE and SSW-NNE directions (FOUNTOULIS 1994, LEKKAS et al. 2000). The Bay of Aghios Andreas and the nearby Katakolo Promontory lie in the midst of the N-S running Elis Graben (EG) system (IGMR 1980) which marks the southward prolongation of the Amfilochia-Etoliko rift zone in southwestern mainland Greece. The area is made up of Neogene siltstones and marls outcropping along the coast north of Aghios Andreas. There are numerous W-E running minor fault zones (LEKKAS et al. 2000). The central EG has subsided since Miocene times (KELLETTAT et al. 1976, KOWALCYK & WINTER 1979) whereas its eastern footwall has been uplifted at least during the Quaternary (STAMATOPOULOS et al. 1988, 1994). Towards the north, Kyllini headland lies in a zone of local halokinetic uplift triggered by thick Triassic gypsum units in the deeper subground (UNDERHILL 1988, 1989, MARIOLAKOS et al. 1991, MAROUKIAN et al. 2000).

Geomorphological studies on relative sea level changes as well as continuous GPS monitoring of crustal movements along the western Hellenic Arc revealed that the Akarnanian block including the Bay of Aghios Nikolaos, the Ionian Islands as well as the Elis coastal plains are subject to gradual subsidence (VÖTT 2007, HOLLENSTEIN et al. 2006, 2008a).

As for Cefalonia and Strofades Island, considerable uplifting impulses were observed in combination with seismic events (PIRAZZOLI et al. 1994, STIROS et al. 1994, PETER 2001, HOLLENSTEIN et al. 2008b, see also LAGIOS et al. 2007).

### 3 *Methods*

In this paper, we present stratigraphic data of vibracores and sediment outcrops along coastal sections of the Bays of Aghios Nikolaos (Akarnania), Langadakia (Paliki Peninsula, Cefalonia), and Aghios Andreas (western Peloponnese). Vibracoring was performed using an Atlas Copco mk1 corer and a hydraulic lifter; maximum coring depth was 4 m below surface (m b.s.) using core diameters of 6 and 5 cm. Vibracores were photographed, described and sampled in the field. On-site description comprised geomorphological, sedimentological and palaeontological criteria such as grain size distribution, grade of sorting, sediment colour, carbonate contents, and determination of both species and state of preservation of macrofossil remains.

In the laboratory, sediment samples from vibracores were analysed for standard geochemical parameters such as electrical conductivity, pH-value, loss on ignition, and concentrations of (ortho-)phosphate and calcium carbonate. In previous palaeotsunami studies, analyses of microfaunal assemblages helped to detect allochthonous impact on the palaeoenvironmental record, and geophysical techniques were applied for a better interpolation between vibracore data (e.g. VÖTT et al. 2009a, 2009b). Beachrock-type sediments outcropping along the coast were sampled for micromorphological and sedimentological analyses based on thin sections using a polarized microscope (type Leitz Laborlux 12 Pol and Zeiss Axiolab Pol 0.4) and a connected digital camera (type Leica DFC 420). Thin section analysis was also carried out for selected vibracore segments. We used a differential GPS system (type Leica SR 530) to determine the position and elevation of each coring site and sediment outcrop.

This paper deals with the phenomenon of cemented tsunami deposits and the description of elementary geomorphological, sedimentary and micromorphological characteristics. Dating approaches were carried out to verify the young age of the studied material and/or for comparison with existing local tsunami geochronologies (VÖTT et al. 2006, 2007, 2008, 2009a, 2009b). We are aware that radiocarbon dating of samples out of tsunamigenically reworked material yield sheer maximum ages and that, therefore, age inversions in the local geochronostratigraphy occur as a rule; in this case, the youngest age obtained renders the best-fit *terminus ad* or *post quem* for the sedimentary event. Where possible, we used  $^{14}\text{C}$  AMS analyses in combination with the OSL technique. Geoarchaeological findings turned out to be highly valuable for dating issues and cross-checks. Calendar ages were calculated from conventional radiocarbon years by means of the calibration software Calib 5.0.2 (see HUGHEN et al. 2004, REIMER et al. 2004). Marine samples were corrected for an average reservoir effect of 402 years (REIMER & MCCORMAC 2002) although the marine palaeoreservoir effect might not have been constant through time and probably was subject to local variations (see GEYH 2005). X-ray diffraction analyses were carried out for radiocarbon samples from the Bay of Langadakia in order to evaluate potential recrystallisation

effects. On Cefalonia Island and in the western Peloponnese, a 3D laser scanner instrument (LIDAR) was used for topographic measurements and 3D-visualisation of dislocated boulders and beachrock-type calcarenitic layers. The LIDAR instrument (type Riegl TLS LMS-Z420i, accuracy ca. 6 mm) was used in combination with a high-resolution digital camera (type Nikon D200). Point clouds were geo-referenced by means of DGPS (type Topcon HiPer Pro Precise) with an accuracy of 1 cm.

#### 4 *Beachrock-type tsunamites in the Bay of Aghios Nikolaos (Akarnania)*

##### 4.1 *Multiple tsunami landfall in the Agh. Nikolaos coastal zone since the mid-Holocene – a review*

During the past years, intense geo-scientific studies have brought to light manifold evidence of multiple tsunami impact on the coasts between the cities of Lefkada and Preveza in northwestern Greece. The most important findings comprise (i) high-energy washover fans and extensive plains, up to 1.2 km long, in the northern Sound of Lefkada (VÖTT et al. 2009a), (ii) dislocated boulders, up to 5–15 m<sup>3</sup> in volume, found both over and under water towards the east of a former strandline called Plaka (VÖTT et al. 2008), (iii) fields of scattered blocks and stones from the littoral zone found on top of the Cheladivaron Promontory up to 14.80 m above present mean sea level (m a.s.l., VÖTT et al. 2006), (iv) run-up deposits along the western shores of Actio Headland, the Phoukias sand spit and the inner Bay of Aghios Nikolaos with erosional contacts at their bases, rip-up clasts and shell debris layers including numerous articulated specimens of marine molluscs in overall fining upward sequences up to 6.70 m a.s.l. (VÖTT et al. 2006, MAY et al. 2007, see also DONATO et al. 2008). Further tsunami traces are (v) coarse-grained breakthrough sediments across the N-S trending Aghios Nikolaos bedrock sill separating the Lake Voulkaria freshwater environment from the open sea, tsunamigenic suspension deposits in the lake's profundal zone and layers of allochthonous sand, gravel and shell debris intersecting autochthonous limnic to swampy deposits along its shores (VÖTT et al. 2006, 2009b). Additional evidence is given by (vi) layers of coarse-grained allochthonous material from marine origin multiply intercalated in autochthonous shallow-water lagoonal mud all along the 4.5 km-long central Sound of Lefkada (VÖTT et al. 2009a).

High-energy deposits encountered in the Aghios Nikolaos coastal zone cannot be interpreted as storm deposits as they were accumulated far beyond the range of storm events especially in the remote and sheltered areas of the Lake Voulkaria and the inner Sound of Lefkada. Moreover, results from relative sea level studies along the coasts of Akarnania and Lefkada Island (VÖTT 2007) show that, during the entire Holocene, sea level has never been higher than the present one; allochthonous high-energy deposits found way above present sea level can therefore not be taken as sea level highstand markers. For detailed discussion and further geomorphological, sedimentological and geoarchaeological characteristics of tsunami-borne deposits see VÖTT et al. (2006, 2008, 2009b) for the Bay of Aghios Nikolaos and the Lake Voulkaria, MAY et al. (2007) and VÖTT et al. (2007) for Actio Headland and the Phoukias sand spit, and VÖTT et al. (2009a) for the Sound of Lefkada.

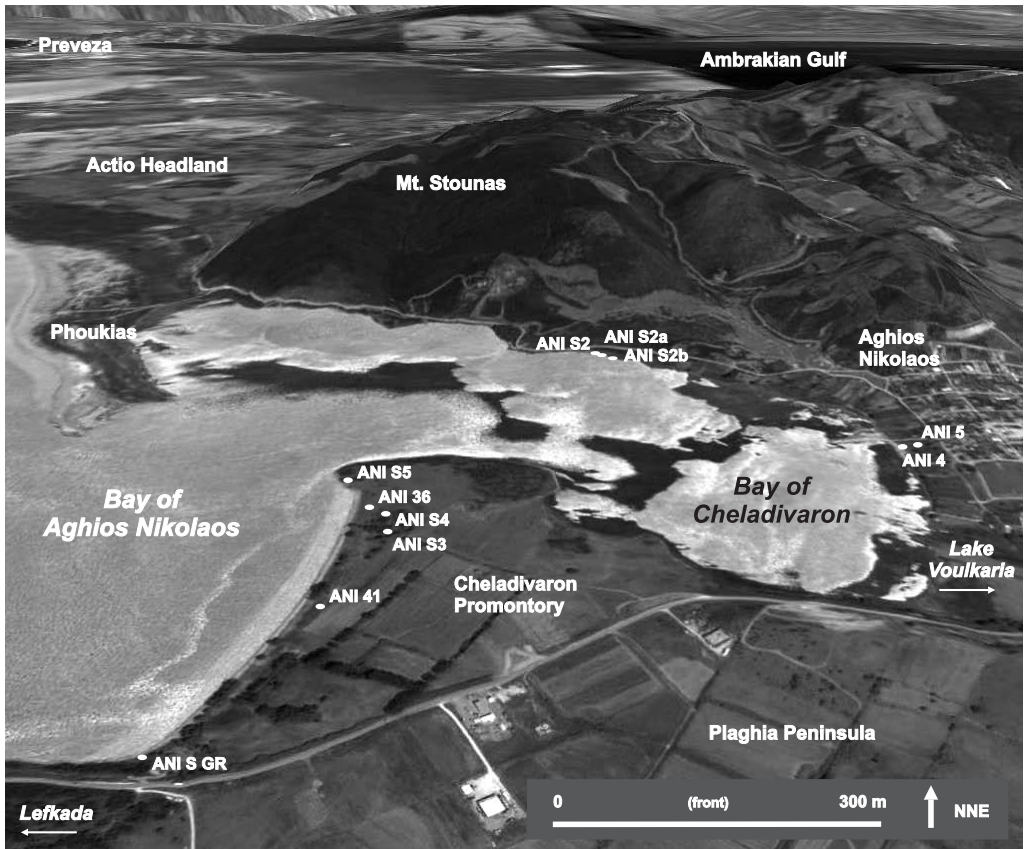


Fig. 2. Bird's eye view of the Bay of Aghios Nikolaos. The Lake Voulkaria is located to the east of the Aghios Nikolaos bedrock sill at the right margin. Digital elevation model and satellite image from Google Earth, vertical exaggeration 3x. View direction towards the NNE.

The local geochronostratigraphy of tsunami imprint shows major impacts for the early 6<sup>th</sup> millennium BC, for the time around 2800 cal BC, around 1000 cal BC, the 4<sup>th</sup>/3<sup>rd</sup> century BC, and between 1000–1400 cal AD (VÖTT et al. 2006, 2007, 2008, 2009a). Moreover, for the first time in northwestern Greece, it was possible to find traces of the 365 AD mega tsunami caused by a strong earthquake near Crete (VÖTT et al. 2009b). Altogether, we found an approximate re-occurrence interval for major destructive tsunamis of around 500–1000 calendar years.

Tsunami modelling approaches based on the open source AnuGa software developed by Geoscience Australia and the Australian National University yielded good accordance with the spatial distribution pattern of tsunami deposits (FLOTH et al. 2009). We found that tsunami wave propagation and runup are strongly influenced by the funnel-shaped coastline configuration in the Lefkada-Preveza coastal zone. Based on this amplifying effect, the region turned out to be extremely sensitive to tsunami wave impact, at the same time offering a large number of high-resolution tsunami sediment traps.

In this paper, we present geo-scientific data from the northern shore of the Bay of Aghios Nikolaos and from the Cheladivaron Promontory separating the inner embayment (= Bay of Cheladivaron) from the outer bay (Fig. 2). The entire bay is protected from open sea wave dynamics by the S-N running Plaka beach ridge ruin, a natural breakwater lying some 3.5 km to the west of the promontory.

4.2 The northern shore

We present stratigraphic and micromorphological data from three outcrops from the northern shore of the Bay of Aghios Nikolaos (ANI S2, S2a, S2b) in combination with new data from two vibracores (ANI 4, 5) that were already discussed in a previous paper (VÖRTT et al. 2006; Figs. 2 and 3).

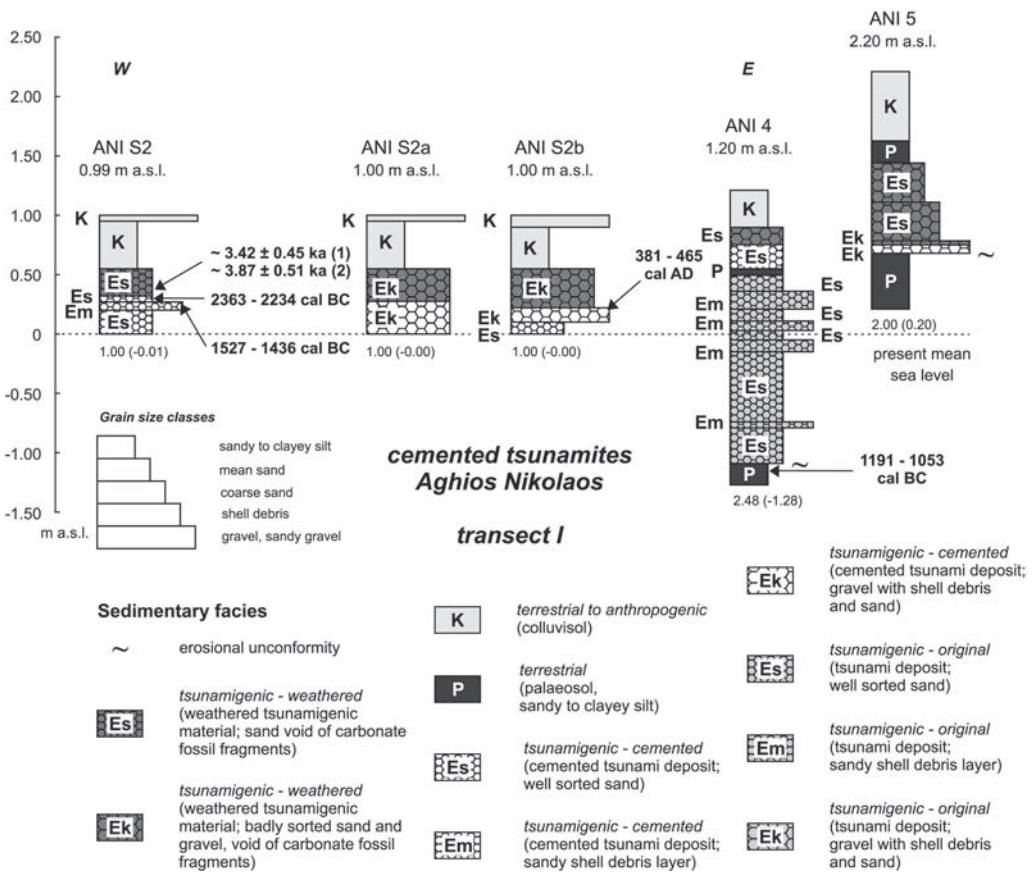


Fig. 3. Stratigraphies and vertical facies distribution of coastal calcarenitic outcrops and vibracores of transect I along the northern shore of the Bay of Aghios Nikolaos (for location of transect see Figs. 1 and 2).

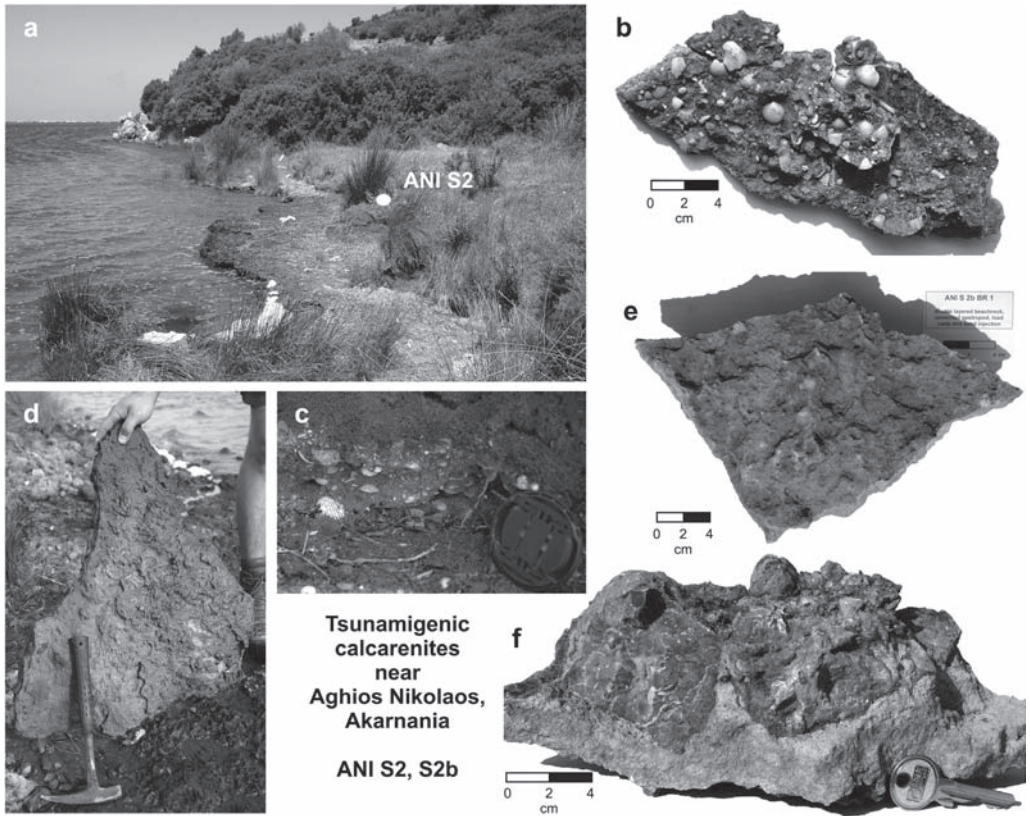


Fig. 4. Beachrock-type tsunami deposits on the northern shore of the Bay of Aghios Nikolaos (Akarnania). (a) General view of the calcarenitic tsunamite around site ANI S2. Decalcified and subsequently oxidized brown tsunami sands on top of the cemented crust are largely eroded and form a small cliff some 2–5 m inland from the waterfront; (b) cemented sandy shell debris layer of profile ANI S2 (0.19–0.26 m a.s.l.) in which the majority of mollusc shell valves are encrusted with their convex side facing upwards; (c) analogous to (b) but with crust in in-situ position and covered by decalcified tsunami sand; (d) bottom side of tsunamite at site ANI S2b (0.01 m b.s.l.). Where the carbonate crust is scoured gastropods such as *Gibbula* sp. are grazing for diatoms and algae (20 cm below thumb); (e) load casts at the bottom side of cemented tsunamigenic sands at ANI S2b (0.01 m b.s.l.); (f) load casts and weak injection structures at the transition from the lower sand-dominated to the upper coarse-grained tsunamite section at site ANI S2b (0.09 m a.s.l.). Photos taken by A. Vött, 2007, 2008.

#### 4.2.1 Sedimentary evidence from coastal calcarenitic outcrops and vibracores

Coastal calcarenitic outcrops ANI S2, S2a and S2b are located some 0.5 km to the north-west of the inner harbour. The three profiles lie at the immediate waterfront within a distance of 50 m (Figs. 2 and 4a).

Profile ANI S2 (N 38°52'34.687", E 20°47'24.554", ground surface 0.99 m a.s.l.) shows a thick carbonate crust out of well sorted sand (0.01 m below sea level (m b.s.l.) – 0.19 m

a.s.l. and 0.26–0.31 m a.s.l.) sandwiching a cemented sandy shell debris layer (0.19–0.26 m a.s.l.) in which the majority of mollusc shell valves are encrusted with their convex side facing upwards (Figs. 3, 4a, 4b and 4c). The upper part of the profile is made out of decalcified brown sand (0.31–0.54 m a.s.l.), representing a palaeosol, and overlain by two colluvisol units (0.54–0.99 m a.s.l.). The lower colluvisol unit consists of sandy to clayey silt whereas the upper unit additionally shows abundant gravel and stones partly originating from the littoral zone as evidenced by marine bio-erosion features.

Profile ANI S2a (ground surface 1.00 m a.s.l.) is characterized by a well cemented layer of badly sorted sandy gravel and stones including marine macrofaunal fragments (0.01 m b.s.l. – 0.21 m a.s.l.). It is followed by the same material but in a non-cemented constellation and void of fossil shells (0.21–0.54 m a.s.l.). The top of the profile shows the same colluvisol units as encountered at ANI S2.

The base of profile ANI S2b (ground surface 1.00 m a.s.l.) is characterized by cemented sand (0.01 m b.s.l. – 0.09 m a.s.l.) covered by cemented sandy gravel and stones up to 15 cm in diameter (0.09–0.21 m a.s.l.), also including macrofossil remains of a marine fauna. The basal sand crust shows clear load cast structures (Figs. 4d and 4e). Load casting combined with weak injection of sandy material from the underlying unit can also be observed for the cemented gravel unit (Fig. 4f). The carbonate crust is covered by non-cemented sandy gravel (0.21–0.54 m a.s.l.). The upper colluvisol units are identical to the ones of profiles ANI S2 and ANI S2a.

Vibracore profile ANI 4 (N 38°52'8.520", E 20°48'4.860", ground surface 1.20 m a.s.l.) shows several grey to brownish grey fining upward sequences out of sand (1.10–0.43 m b.s.l.) on top of an erosional contact formed in a clayey to silty palaeosol. The sandy sequences mostly start with a shell debris layer including coarse sand and few pieces of gravel, then turn into mean and further up-core into fine sand which is partly laminated. The following brown palaeosol (0.43–0.54 m a.s.l.) is covered by a white crust of cemented sand and shell debris (0.54–0.74 m a.s.l.). The latter is overlain by brown sand including few pieces of gravel (0.74–0.85 m a.s.l.). The uppermost part of the profile is a brown, sandy to loamy colluvisol (0.85–1.20 m a.s.l.).

Vibracore ANI 5 (N 38°52'9.540", E 20°48'6.120", ground surface 2.20 m a.s.l.) also shows an erosional unconformity in the basal palaeosol. The following fining upward sequence of gravel and marine mollusc fragments (0.67–0.74 m a.s.l.) is covered by brown coarse and mean sand (0.74–1.25 m a.s.l.). The top section of the profile is characterized by a palaeosol and a subsequent colluvisol (1.25–2.07 m a.s.l., see also VÖTT et al. 2006).

#### 4.2.2 Evidence from thin section analysis

Thin section analyses were conducted for samples from the cemented parts of profiles ANI S2, S2a and S2b (Fig. 5) as well as from the carbonate crust and the overlying sand layer encountered in the upper part of vibracore ANI 4 (Fig. 6).

The cemented marine sand found in profile ANI S2 is comparatively well sorted containing several foraminifers (Fig. 5a, upper center and right center) and large fragments

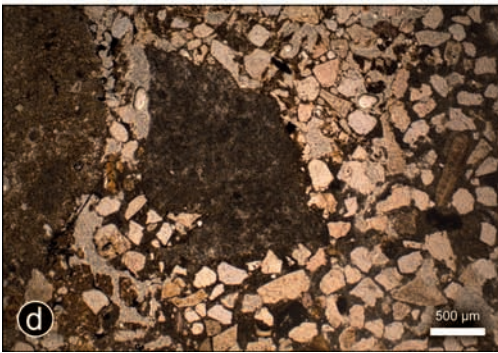
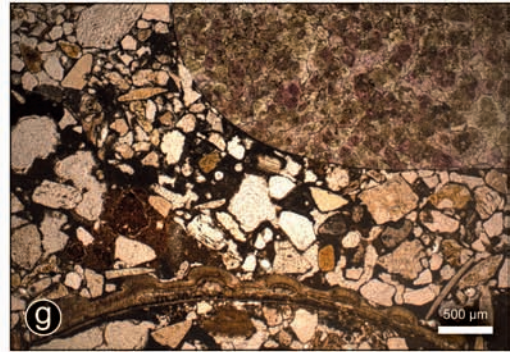
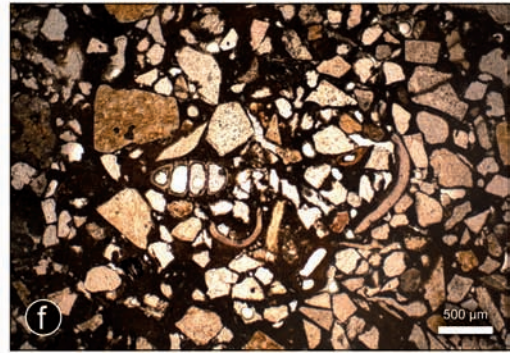
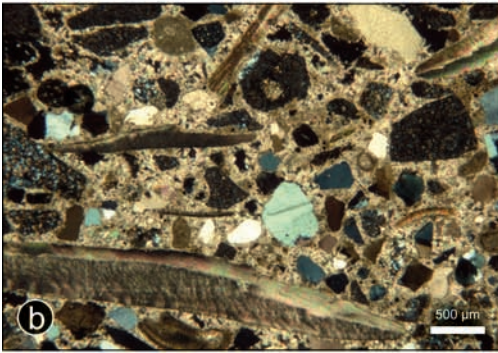
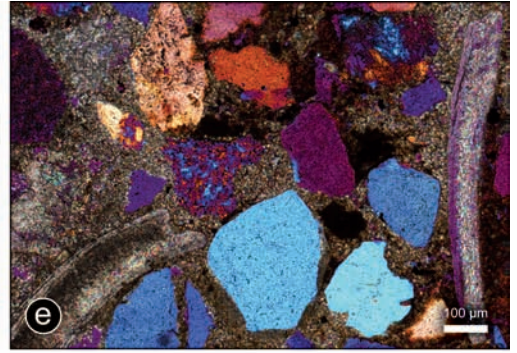
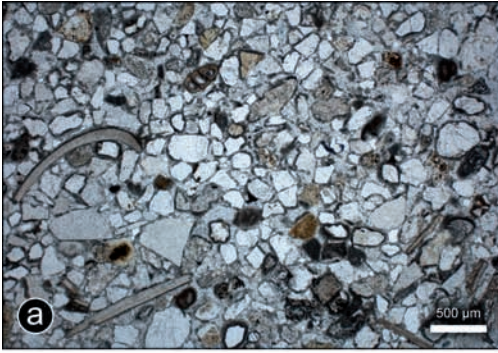




Fig. 5. Thin sections of calcarenitic tsunamites from the northern shore of the Bay of Aghios Nikolaos. See Figs. 1 and 2 for locations of sampling sites, Fig. 3 for stratigraphic positions of thin sections, and text for further explanations. PPL – plain polarized light, +N – crossed Nichols. (a) ANI S2 BR1 (0.26–0.31 m a.s.l.), PPL; (b) ANI S2 BR2 (0.19–0.26 m a.s.l.), +N; (c) ANI S2 BR3 (0.15–0.19 m a.s.l.), PPL; (d) ANI S2a BR1 (0.16–0.21 m a.s.l.), PPL; (e) ANI S2a BR2 (0.11–0.16 m a.s.l.), +N; (f) to (h) ANI S2b BR1 (-0.01–0.09 m a.s.l.), PPL.

of marine fossils (Figs. 5a and 5c). However, there are abundant angular and even sharply edged mineral grains (Figs. 5a, 5b and 5c) documenting that the material was not subject to steady transport and rounding as known from the littoral zone. The cemented sand and shell debris layer of ANI S2 also shows a lot of flake-like mineral grains and shell debris fragments while the overall appearance is fairly unsorted (Fig. 5b). Further, numerous grains are oxidized and thus appear brownish (Fig. 5a). Other grains show micro-crystals of pyrite documenting that they were, for a long time, subject to anoxic conditions before deposited at site ANI S2 (Fig. 5c, center).

As for profile ANI S2a, mineral grains appear strongly edged and partly even broken into pieces (Fig. 5e, lower left). The ANI S2a crust comprises both well rounded pieces of gravel (Fig. 5d, upper left) and flake-type sand grains (Fig. 5d, center).

Thin sections from the basal sand unit encountered in the cemented parts of ANI S2b reveal that large parts of the material are of marine origin, e.g. by foraminifer findings (Fig. 5f, center) and large macrofossil fragments (Figs. 5g and 5h). However, the deposits show an overall unsorted and rather chaotic structure (Fig. 5g). We also found mollusc shell fragments that were obviously broken at several points in the very course of the sedimentation process (Fig. 5h).

The carbonate crust found in vibracore ANI 4 (Figs. 6b to 6d) is characterized by a mixture of angular to edged mineral grains of terrestrial origin (Fig. 6c, lower center), partly oxidized, and shell debris, echinoid spine fragments (Fig. 6b, upper left), and rounded mineral grains of littoral to marine origin. Some quartz grains show sharp and fresh fractures and appear to be broken shortly before cemented by the carbonate matrix (Fig. 6d). By comparing the sedimentary structure of the lithified allochthonous marine deposits of core ANI 4 (Figs. 6b to 6d) with the overlying brown sand (Fig. 6a) we suggest that the latter has been formed by dissolution of the carbonate shell fragments by percolating waters because the mineral grain skeletons of the two deposits are completely identical (compare Figs. 6a and 6b). The high proportion of 30–40 % porosity of the brown sand clearly supports this scenario (Fig. 6a).

#### 4.3 *The Cheladivaron Promontory*

From the western shore of the Cheladivaron Promontory, we present data from two near-shore (ANI S3, ANI S4) and two coastal calcarenitic outcrops (ANI S GR, ANI S5) as well as the stratigraphies of two vibracores (ANI 36, ANI 41, Figs. 2 and 7).

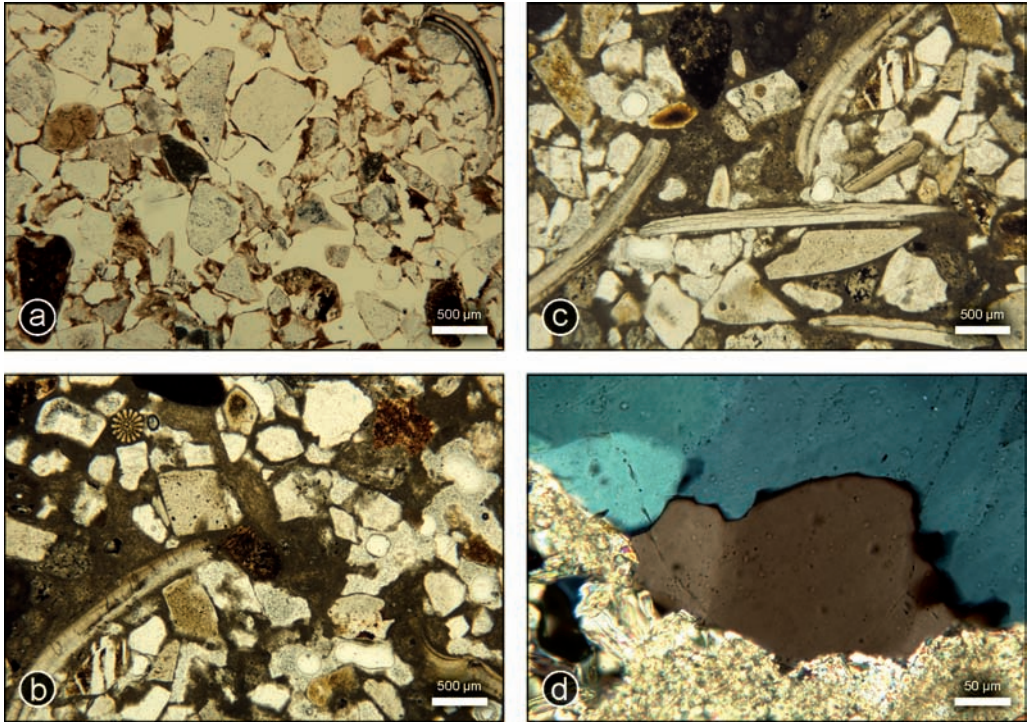


Fig. 6. Thin sections of cemented tsunamites encountered in vibracore profile ANI 4 drilled at the northern shore of the Bay of Aghios Nikolaos. See Figs. 1 and 2 for location of the vibracoring site, Fig. 3 for stratigraphic positions of thin sections, and text for further explanations. PPL – plain polarized light, +N – crossed Nichols. (a) ANI 4/2+ (0.76 m a.s.l.), PPL; (b) and (c) ANI 4/3 (0.67 m a.s.l.), PPL; (d) ANI 4/3 BR/DS (0.64 m a.s.l.), +N.

#### 4.3.1 Evidence from profile outcrops and vibracores

Near-shore profiles ANI S3 (N 38°52'2.870", E 20°47'26.564", ground surface 6.90 m a.s.l.) and ANI S4 (N 38°52'3.874", E 20°47'25.844", ground surface 5.85 m a.s.l.) are located some 60–70 inland on the western flank of a small rocky hilltop. Both profiles show a clear erosional discontinuity on top of local Triassic bedrock followed by a thick and well cemented layer (ANI S3: 5.60–6.10 m a.s.l., ANI S4: 5.50–5.80 m a.s.l.) of both well rounded gravel and angular stones (Figs. 7, 8b and 8c) in a sandy matrix with numerous fragments of a marine macrofauna (Fig. 8c). In this unit, we also found ripped-up and incorporated stones with boreholes from *Lithophaga* sp. indicating the marine origin of the material (Fig. 8c, inset). Subsequently, a sand-dominated calcarenite follows, rich in shell fragments (ANI S3: 6.10–6.60 m a.s.l.). Its uppermost part is weathered and characterized by soil formation (ANI S3: 6.60–6.90 m a.s.l., ANI S4: 5.80–5.85 m a.s.l.; Figs. 7 and 8b).

Profile ANI S GR is located at the southern end of the promontory on the immediate waterfront (N 38°51'49.470", E 20°47'15.260", ground surface 0.30 m a.s.l.). It is made

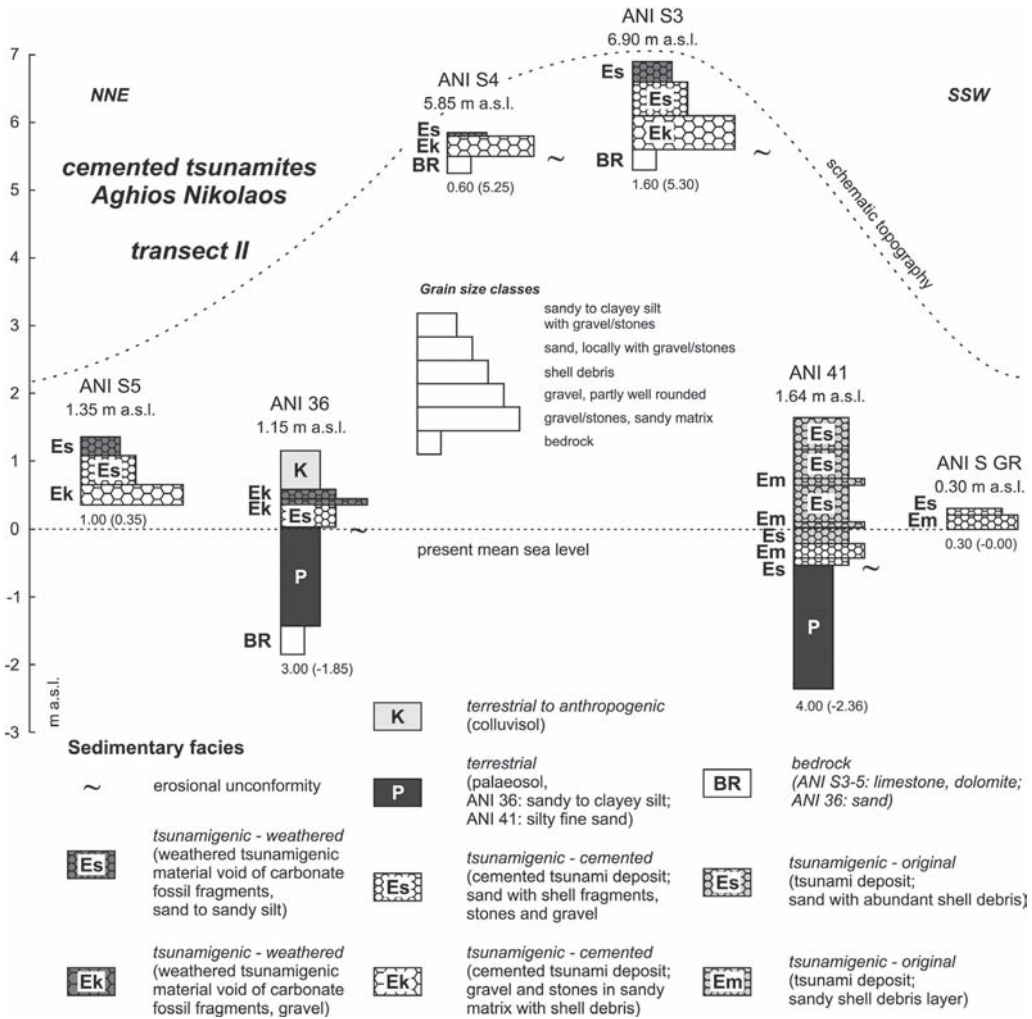


Fig. 7. Stratigraphies and vertical facies distribution of near-shore and coastal calcarenitic outcrops and vibracores of transect II along the western shore of the Cheladivaron Promontory (for location of transect see Figs. 1 and 2).

out of a 20 cm-thick unit of cemented sandy shell debris with abundant fragmented and articulated molluscs (0–0.20 m a.s.l.). The following cemented sand layer is still rich in fossil fragments (0.20–0.30 m a.s.l.). The ANI S GR crust partly encloses large boulders, up to 2 m in diameter, which originate from Triassic bedrock outcrops further upslope.

Profile ANI S5 is located at the opposite flank of the promontory some 600 m further north (N 38°52'7.698", E 20°47'23.975", ground surface 1.35 m a.s.l.). Its base shows cemented gravel and stones in a sandy matrix also including shell fragments (0.35–0.65 m a.s.l.) and followed by a similar, but sand-dominated section (0.65–1.08 m a.s.l., Figs. 8d

and 8e). The uppermost part of the profile is made out of decalcified sand (1.08–1.35 m a.s.l.); numerous blocks and stones from the littoral zone were found lying on the terrain surface.

Vibracoring site ANI 36 is located right in between sites ANI S4 and ANI S5 around 30 m inland (N 38°52'5.067", E 20°47'24.712", ground surface 1.15 m a.s.l.). Its base is characterized by a palaeosol (1.43 m b.s.l. – 0.03 m a.s.l.) on top of older sandy deposits. We found a sharp erosional contact towards the following layer of cemented sand the latter including abundant shell debris and also black limestone fragments (0.03–0.35 m a.s.l.). The subsequent weathered coarse-grained gravelly deposits (0.35–0.44 m a.s.l.) are, further up-core, covered by sand (0.44–0.58 m a.s.l.) including well rounded pieces of pumice and singular limestone fragments with signs of marine bio-erosion. The top of the profile shows a colluvisol (0.58–1.15 m a.s.l.).

Vibracore ANI 41 (N 38°51'57.622", E 20°47'22.226", ground surface 1.64 m a.s.l.) was drilled some 230 m to the south-southeast of site ANI 36 on top of a ridge-type morphological unit with tongue-like lobes showing towards inland. On top of an erosional contact, we found thick marine deposits (0.53 m b.s.l. – 1.17 m a.s.l.) with three well discernible fining upward sequences. Each sequence starts with a shell debris layer plus sand and partly also pieces of well rounded gravel followed by mean sand with an increasing amount of fine sand towards the top. The lowermost part of the marine sequence is well cemented (0.53–0.21 m b.s.l.) and revealed numerous mollusc valves regularly adjusted with their convex side facing upwards (see profile ANI S2, Section 4.2.1). The uppermost part of core ANI 41 consists of decalcified brown fine sand (1.17–1.64 m a.s.l.).

#### 4.3.2 Evidence from thin section analysis

Micromorphological studies were carried out for samples from profiles ANI S GR, ANI S3, ANI S5 as well as from vibracore ANI 36.

Concerning profile ANI S GR, mineral grains are mainly restricted to the upper stratigraphic unit (Fig. 9a). Many grains show pyrite crystals (Fig. 9a, center right) or coatings of iron oxide (Fig. 9a, center left) and thus indicate anoxically subaqueous and terrestrial areas of origin, respectively. Thin sections from the lower unit of profile ANI S GR reveal large shell fragments, partly adjusted and embedded in a carbonate matrix, as well foraminifers (Fig. 9b, center, presumably remains of the benthic shallow water species *Ammonia beccarii*). The high porosity visible in the ANI S GR thin sections reflects gradual dissolution of the crust by subaerial weathering.

We found cracked pieces of black limestone in thin sections of the coarse-grained unit of profile ANI S3. Fig. 9c (upper left) clearly depicts the lateral shearing of a limestone fragment into pieces as well as the occurrence of sharply edged limestone flakes (Fig. 9c, center) in direct combination with shell and foraminifer fragments (Fig. 9d, lower right). This testifies to strong impact from the marine side. In many cases, limestone surfaces are characterized by sequences of concave impact marks (Fig. 9c, right center and Fig. 9d, upper center).

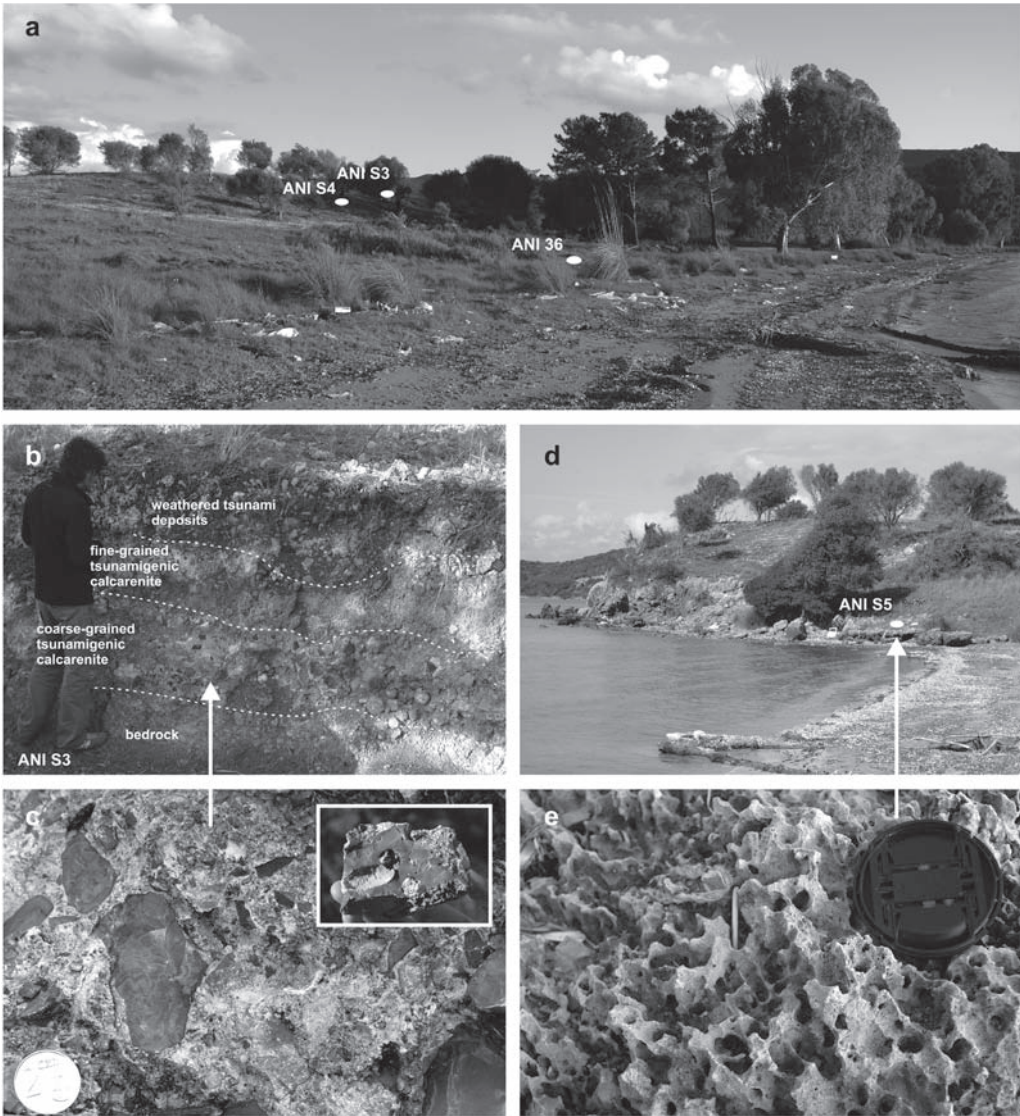


Fig. 8. Beachrock-type tsunami deposits along the western shore of the Cheladivaron Promontory (Akarnania). (a) General view of the central Cheladivaron Promontory with locations of vibracoring site ANI 36 and outcrops ANI S3 and S4; (b) tsunamite outcrop in near-shore profile ANI S3 on the western flank of a small rocky hill; (c) detail of lowermost section of profile ANI S3 showing angular intra-clasts, partly with signs of bio-erosion by littoral zone boring organisms (see inset), and shell debris in a sandy matrix; (d) beachrock-type tsunami deposit at site ANI S5; (e) detail of cemented tsunami sands at site ANI S5 (0.65 m a.s.l.), strongly karstified. Photos taken by A. Vött, 2007, 2008.

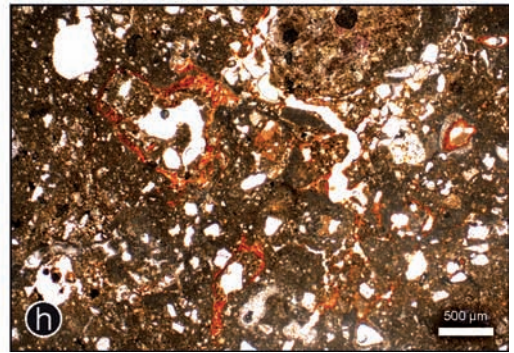
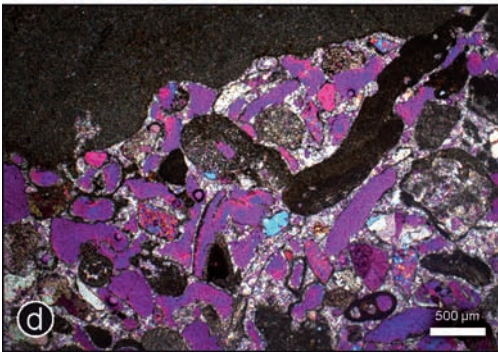
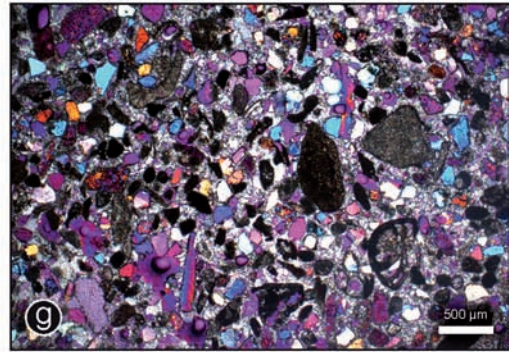
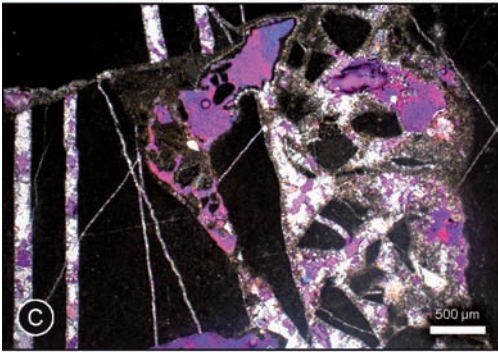
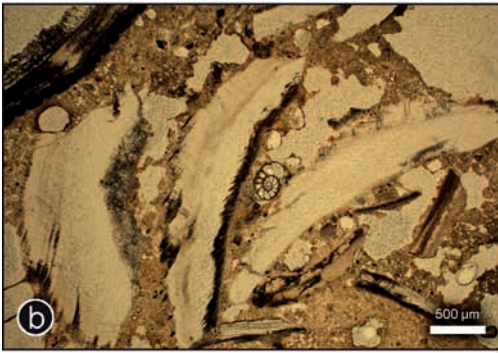
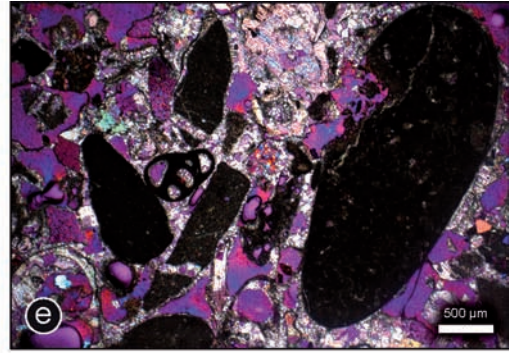
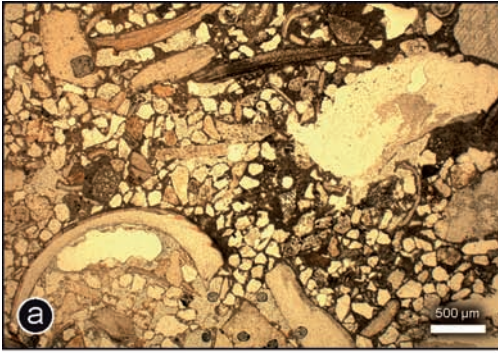




Fig. 9. Thin sections of calcarenitic tsunamites from the western flank of the Cheladivaron Promontory. See Figs. 1 and 2 for locations of sampling sites, Fig. 7 for stratigraphic positions of thin sections, and text for further explanations. PPL – plain polarized light, +N – crossed Nichols. (a) ANI S GR2 (0.25 m a.s.l.), PPL; (b) ANI S GR1 (0.15 m a.s.l.), PPL; (c) and (d) ANI S3 BR1 (6.10 m a.s.l.), +N; (e) ANI S3 BR2 (5.66 m a.s.l.), +N; (f) ANI S3 BR4 (6.60 m a.s.l.), PPL; (g) ANI S5 BR2 (0.50 m a.s.l.), +N; (h) ANI S5 BR4 (1.08 m a.s.l.), PPL.

Well rounded pebbles from the littoral zone are associated to angular and even flake-type limestone fragments, individual pebbles being partly smashed by impacting forces (Fig. 9e, center right). These micromorphological features clearly document high to even extreme energy influence on the site. Similar micromorphological characteristics were found by BRUZZI & PRONE (2000) for quartz grains which were subject to mechanical impact within the course of tsunami and storm events. Thin sections from the fine-grained upper unit of profile ANI S3 reveal abundant shell fragments, partly adjusted in a parallel way and associated to angular and partly oxidized mineral grains (Fig. 9f, center left). Due to the high elevation of this part of the profile, dissolution of the carbonate cement by percolating rain-water has already produced a comparatively high porosity.

Thin sections from the lower parts of profile ANI S5 show an unsorted mixture of shell and foraminifer debris associated to both angular and rounded mineral grains (Fig. 9g). In contrast, samples from the uppermost section of the profile reveal a dense carbonate crust with only few mineral grains (Fig. 9h). The crust, however, is subject to dissolution and subsequent oxidation along root channels (Fig. 9h, center).

The cemented layer encountered in vibracore ANI 36 is made up of a fairly unsorted mixture of mineral grains and shell debris (Fig. 10a). Its uppermost section, however, is already in state of dissolution. Shell fragments are fairly well adjusted and associated to mineral grains and foraminifers (Fig. 10b). Similar to the situation observed in profile ANI S2b (Fig. 5h), rapid deposition of the entire sedimentary unit as a whole induced destruction of shell remains, in this case the valves of an indeterminable ostracod (Fig. 10c, center). Mineral grains are often sharply edged (Fig. 10d, lower center), some of them showing oxidic coatings indicating a terrigenous origin (Fig. 10d, upper left and center right).

#### 4.4 *Post-sedimentary pedogenetic cementation*

Fig. 11 depicts carbonate contents (in weight-%) analysed for sediment samples from cores ANI 4, 5, 36 and 41 compared to simplified facies profiles. It can be seen that the basal palaeosol units are, at least in their uppermost part, completely void of carbonate. In every core, the onset of allochthonous marine deposits is represented by an abrupt increase in the carbonate content. However, vertical carbonate profiles of ANI 5, 36 and 41 document strongly but steadily increasing carbonate concentrations within the marine sequence from top to bottom. Highest values were found for the carbonate crusts themselves with maximum 51 % at ANI 5, up to 29 % at ANI 36 and almost 67 % at ANI 41. Considering

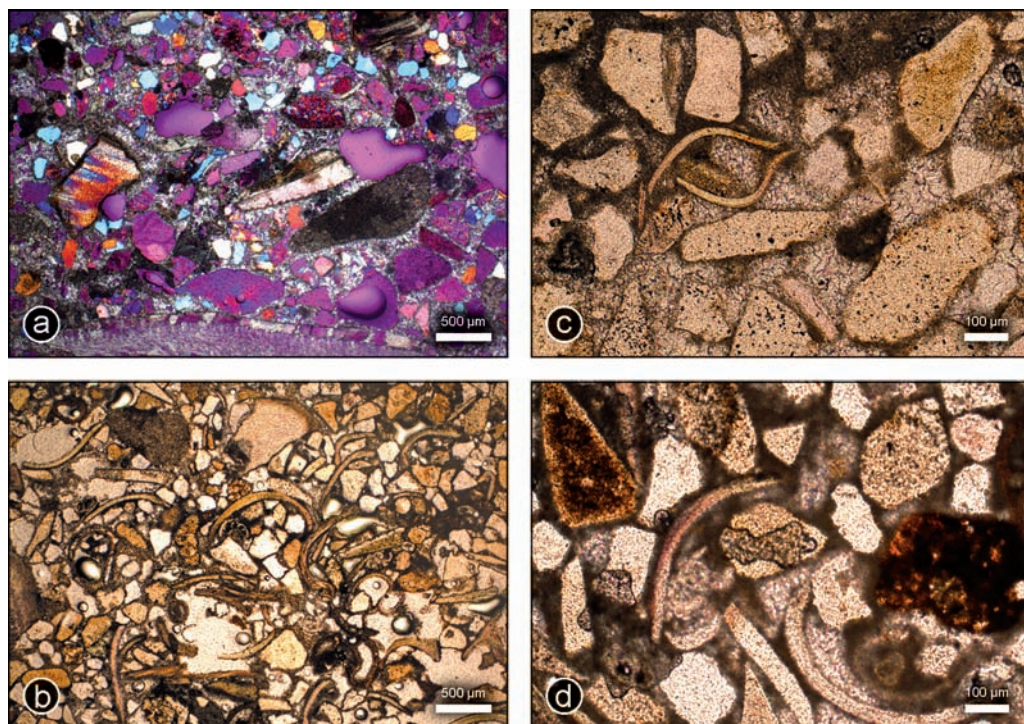


Fig. 10. Thin sections of cemented tsunamites encountered in vibracore profile ANI 36 drilled at the western shore of the Cheladivaron Promontory. See Figs. 1 and 2 for location of the vibracoring site, Fig. 7 for stratigraphic positions of thin sections, and text for further explanations. PPL – plain polarized light, +N – crossed Nichols. (a) ANI 36/5 KK (0.19 m a.s.l.), +N; (b) ANI 36/6 KK (0.08 m a.s.l.), PPL; (c) ANI 36/6 ST/KK (0.12 m a.s.l.), PPL; (d) ANI 36/6+ KK (0.03 m a.s.l.), PPL.

amounts of annual precipitation in northwestern Greece reaching up to 800–1200 mm (LIENAU 1989), crust formation is best explained by carbonate dissolution and subsequent oxidation of upper sand units and downward transport of dissolved carbonate within the marine sequence. It is known from pedogenetic studies that recrystallisation will take place in or slightly above groundwater level due to the rapid change of the solubility product and/or where a strong decrease in porosity and thus in percolation capacity occurs (e.g. SCHEFFER & SCHACHTSCHABEL 2002: 455ff.). The latter can be observed in cores ANI 5, 36 and 41 where percolating and carbonate-saturated waters are hindered from further seepage by the clayey to silty palaeosol material underneath the marine sequence. Thus, the lowermost parts of the marine deposits remain fully saturated over a long time so that shell debris may act as initial nucleus for recrystallisation processes. Post-sedimentary pedogenetic decalcification and subsequent cementation are suggested to take place within a considerably short time span after deposition.

Our results and interpretation are supported by the fact that thin sections of both decalcified and encrusted material show completely identical mineral skeletons (Section 4.2.2, see also VÖTT et al. 2009b).

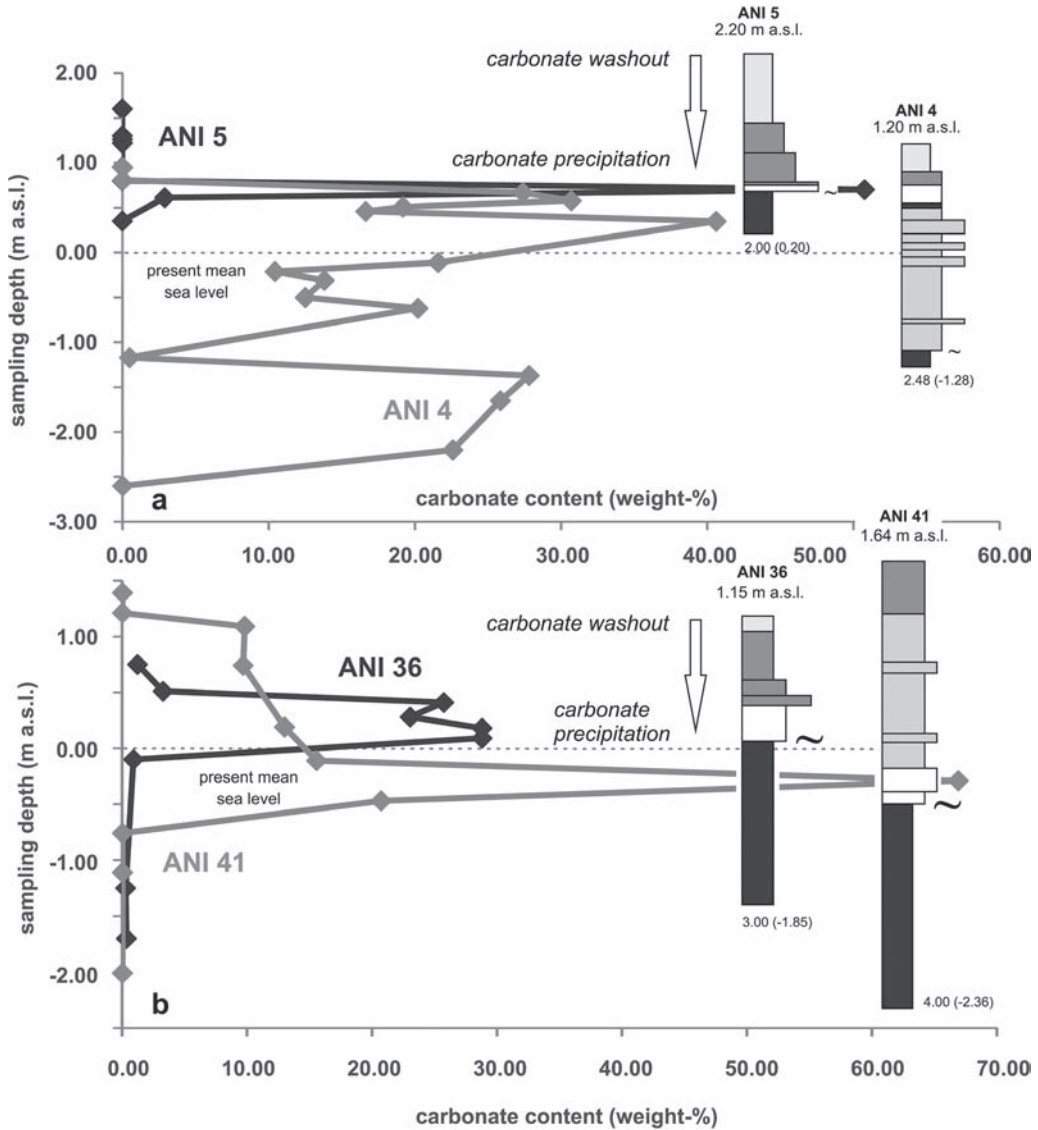


Fig. 11. Vertical profiles of carbonate contents analysed for vibracores ANI 4 and 5 drilled at the Aghios Nikolaos harbour (a) and for vibracores ANI 36 and 41 drilled at the western shore of the Cheladivaron Promontory (b). Simplified stratigraphies of vibracores are adjusted to vertical scale of y-axis; white sections correspond to cemented tsunami deposits. See Figs. 1 and 2 for locations of vibracoring sites.

#### 4.5 Discussion and dating approaches

Based on the sedimentary and micromorphological findings encountered in profiles of transect I (Figs. 3 to 6 and Fig. 10), the following statements can be made. (i) The overall macro- and micro-structure of the cemented sediments clearly indicates high-energy influence. This is all the more striking as recent sedimentary dynamics in the inner Bay of Aghios Nikolaos (= Bay of Cheladivaron) are characterized by anoxic conditions and the accumulation of silty to clayey mud rich in organic matter. (ii) Most prominent high-energy impact features are the high amount of coarse mineral grains and shell fragments, their angular and even flake-like shape as well as fractionating and high-pressure impact structures. (iii) Load cast and injection features cannot be explained by littoral processes. They rather reflect the sudden and non-recurring accumulation of a water-saturated sedimentary unit which subsequently got subject to post-depositional deformation. (iv) A considerable portion of the sediment originates from non-littoral terrigenous and quiescent underwater environments due to signs of subaerial oxidation and anoxic pyrite formation. These findings implicate that, during high-energy impact, littoral but also adjacent terrestrial and lagoonal environments were strongly affected. This kind of sedimentary dynamic is only known for tsunami wave action (e.g. BRUINS et al. 2008, VÖTT et al. 2009a, 2009b). (v) The partly chaotic and unsorted structure on the one hand and the partly laminated and adjusted appearance of the material on the other hand seem to correspond to phases of more turbulent runup and more laminar overflow, respectively, during high-energy tsunami inundation. (vi) From a stratigraphic point of view, ANI S2, S2a, S2b high-energy deposits are stratigraphically well consistent with tsunamigenic layers found in nearby cores ANI 4 and ANI 5 which also appear partly cemented. The ANI S2, S2a, S2b crusts represent the cemented part of a thicker and in its upper section partly weathered unit of allochthonous tsunami deposits.

Concerning transect II profiles (Figs. 7 to 10), the encountered marine sequences are due to high-energy wave impact on the Cheladivaron Promontory. The main arguments are the following. (i) Sharp erosional contacts in basal palaeosols, (ii) multiple fining upward sequences, partly including rip-up clasts, in marine deposits untypical of the present sedimentary environment, and (iii) clear landward and upward thinning of allochthonous deposits are among those sedimentary features found associated to tsunami deposits (DAWSON 1994, DOMINEY-HOWES et al. 2006, DAWSON & STEWART 2007, KORTEKAAS & DAWSON 2007, MORTON et al. 2007). Further findings such as (iv) assemblages of well rounded mineral grains and sharply edged limestone flakes side by side, (v) sediments from terrigenous or subaqueous environments amidst material from littoral sites, and (vi) clear impact marks and shearing traces of large mineral clasts indicate large dimension wave impact reaching far beyond the littoral system (see also BRUZZI & PRONE 2000). Moreover, allochthonous deposits occur in similar stratigraphic positions at different sites but in differing topographic elevations. (vii) Encrusted marine deposits found up to around 7 m a.s.l. document exceptional ex-situ marine influence and are consistent with dislocated blocks and stones from the littoral zone encountered up to 14.80 m a.s.l. on top of the Cheladivaron Promontory as well as with runup deposits at the northern shore of the bay at 6.70 m a.s.l. found during previous investigations (MAY et al. 2007, VÖTT et al. 2006, 2009b). (viii) Allochthonous onshore deposits of predominantly marine origin are consid-

erably thinner at the eastern flank of the Cheladivaron Promontory but reach up to 2 m in thickness in the adjacent inner Bay of Cheladivaron (VÖTT et al. 2009b). This is consistent with flow dynamics of extreme waves coming from the seaside and with local divergence and sediment deposition after the waves have overflowed the promontory (FLOTH et al. 2009, VÖTT et al. 2009b).

Against this background, there is no plausible alternative for explaining allochthonous transect I and II deposits (Figs. 3 to 10) as being caused by strong tsunami impact. Our results show that cementation of tsunami deposits in the Bay of Aghios Nikolaos has taken place by post-sedimentary decalcification and weathering of higher sections on the one hand and downward carbonate transport and recrystallisation in places of slack flow on the other hand. Profiles ANI S2, S2a, S2b, S3 and S5 show stratigraphies identical to those encountered in cores ANI 4, 5, 36 and 41. Therefore, we conclude that the occurrence of carbonate crusts at the waterfront is due to the fact that the easily erodible brown and decalcified sands on top have been washed away by littoral processes. This scenario can be verified at sites ANI S2, S2a and S2b where the upper decalcified sand forms a weak cliff some 2-5 m further inland while the encrusted parts of the tsunami deposits are fairly intact on the immediate shore.

The calcarenitic crusts at sites ANI S2, S2a and S2b correspond to the definition given for “beachrock” *sensu stricto* (e.g. SHORT 2005, TURNER 2005, VOUSDOKAS et al. 2007, BIRD 2008). The beachrock units in the Bay of Aghios Nikolaos are thus the first of their kind described as high-energy tsunami deposits post-sedimentarily encrusted in the course of carbonate washout, vertical carbonate transfer, and post-pedogenetic erosion of overlying decalcified units.

Radiocarbon and OSL dating was accomplished for samples from profiles ANI S2 and ANI S2b for comparison with existing local tsunami geochronostratigraphies (Section 4.1). Two shell samples were taken from the cemented layers of profile ANI S2, sample ANI S2 BR1 from in between the topmost sand crust and sample ANI S2 BR2 from the underlying shell debris layer (Table 1). As these strata represent event deposits, incorporated shell fragments yield simple maximum ages due to reworking of older material. The age inversion documented by the ANI S2 dating results is, therefore, not significant. The youngest age obtained yields the best-fit *terminus ad* or *post quem* for tsunami landfall and sediment deposition. It can thus be stated that site ANI S2 was hit by tsunami wave action at or after 1527-1436 cal BC (Table 1).

A third sample from the stratigraphically identical unit in profile ANI S2b was radiocarbon dated to 381–465 cal AD (Table 1). Based on its adhesion-type appearance, we however assume that the dated gastropod was secondarily cemented to the crust’s surface during a later phase of superficial cementation and does not reflect the time of tsunami sediment deposition.

We carried out OSL analyses of two samples from the layer of decalcified and weathered brown sand right on top of the crust in profile ANI S2 in order to date the time of sediment accumulation as such. Two samples were taken from the same depth. OSL dating yielded fairly identical ages ranging from around 3.26 to 3.88 ka before present depending on the water content which we assumed between 5 and 30 % for the time of deposition

Table 1. Radiocarbon dates of samples from the Bays of Aghios Nikolaos (Akarnania) and Langadakia (Cefalonia Island).  
 Note: b.s. – below ground surface; a.s.l. – above sea level; undet. – undetermined; \* – marine reservoir correction with 402 years of reservoir age;  
 $1\sigma$  max; min cal BP/BC (AD) – calibrated ages,  $1\sigma$ -range; “;” – there are several possible age intervals because of multiple intersections with the  
 calibration curve; Lab. No. – laboratory number, University of Kiel (Kia).

Sample Name	Depth (m b.s.)	Depth (m a.s.l.)	Sample Description	Lab. No. (Kia)	$\delta^{13}\text{C}$ (ppm)	$^{14}\text{C}$ Age (BP)	$1\sigma$ max; min (cal BP)	$1\sigma$ max; min (cal BC)
ANI S2 BR 1	0.68	0.28	fragment of undet. marine bivalve	34579	3.7	4170 $\pm$ 30	4312 - 4183	2363 - 2234*
ANI S2 BR 2	0.75	0.24	fragment of undet. marine bivalve	34580	- 0.1	3555 $\pm$ 30	3476 - 3385	1527 - 1436*
ANI S2b BR 1	0.78	0.21	<i>Gibbula</i> sp., complete	34581	- 2.7	1970 $\pm$ 25	1569 - 1485	381 - 465 AD*
ANI 4/13 PR	2.35	1.15	undetermined plant remains	28883	-10.8	2920 $\pm$ 25	3140; 3002	1191; 1053
LAG K 1/3 RC	-	1.25	valve of <i>Ostrea</i> sp.	34404	0.3	19460 $\pm$ 110	22661 - 22414	20712 - 20465*
LAG K 1/5 RC	-	2.60	fragment of undet. marine gastropod	34405	3.5	20240 $\pm$ 120	23953 - 23581	22004 - 21632*
LAG K 1/6 RC	-	1.75	marine gastropod, undet., complete	34406	0.8	14100 $\pm$ 70	16501 - 16094	14552 - 14145*

Table 2. Luminescence dating results of sediment samples from profile ANI S2. Coarse-grained quartz samples were stimulated by blue light (SAR protocol after MURRAY & WINTLE 2000). Note: ED = equivalent dose, DO = dose rate. OSL ages were calculated for three different scenarios of water content between 5 and 30 % estimated for the time of deposition. Luminescence datings were accomplished in the Marburg Luminescence Laboratory.

Sample ID	Lab. code	Sampling depth (m b.s.)	Grain size ( $\mu\text{m}$ )	U (ppm)	Th (ppm)	K (%)	Water content (%)	ED (Gy)	$D_0$ ( $\text{Gy ka}^{-1}$ )	Age (ka)
ANI S2 OSL1	MR0766a	0.58 – 0.62	125 – 180	0.66 $\pm$ 0.08	0.91 $\pm$ 0.13	0.22 $\pm$ 0.01	5 $\pm$ 5	1.86 $\pm$ 0.05	0.57 $\pm$ 0.07	3.26 $\pm$ 0.38
ANI S2 OSL2	MR0767a	0.58 – 0.62	125 – 180	0.56 $\pm$ 0.08	0.53 $\pm$ 0.19	0.23 $\pm$ 0.01	5 $\pm$ 5	1.84 $\pm$ 0.04	0.53 $\pm$ 0.07	3.48 $\pm$ 0.44
ANI S2 OSL1	MR0766b	0.58 – 0.62	125 – 180	0.66 $\pm$ 0.08	0.91 $\pm$ 0.13	0.22 $\pm$ 0.01	15 $\pm$ 10	1.86 $\pm$ 0.05	0.54 $\pm$ 0.07	3.42 $\pm$ 0.45
ANI S2 OSL2	MR0767b	0.58 – 0.62	125 – 180	0.56 $\pm$ 0.08	0.53 $\pm$ 0.19	0.23 $\pm$ 0.01	15 $\pm$ 10	1.84 $\pm$ 0.04	0.50 $\pm$ 0.07	3.66 $\pm$ 0.52
ANI S2 OSL1	MR0766c	0.58 – 0.62	125 – 180	0.66 $\pm$ 0.08	0.91 $\pm$ 0.13	0.22 $\pm$ 0.01	30 $\pm$ 10	1.86 $\pm$ 0.05	0.51 $\pm$ 0.07	3.63 $\pm$ 0.45
ANI S2 OSL2	MR0767c	0.58 – 0.62	125 – 180	0.56 $\pm$ 0.08	0.53 $\pm$ 0.19	0.23 $\pm$ 0.01	30 $\pm$ 10	1.84 $\pm$ 0.04	0.47 $\pm$ 0.06	3.88 $\pm$ 0.53

(Table 2). OSL dates are well consistent with the calibrated maximum radiocarbon age of the underlying crust given as 1527-1436 cal BC (Table 1). It can thus be concluded that the event deposits encountered in profile ANI S2 were accumulated in the last third of the 4<sup>th</sup> millennium BC.

Our results are in good accordance with a radiocarbon date from profile ANI 4 (Fig. 3) and numerous other dates obtained for samples from the shores and the profundal zone of the nearby Lake Voukaria all of them describing strong tsunami landfall in the Bay of Aghios Nikolaos and its environs around 1000 cal BC (VÖTT et al. 2006, 2009b).

## 5 *Beachrock-type tsunamites in the Bay of Langadakia (Cefalonia)*

Detailed geomorphological and sedimentological studies were carried out in the Bay of Langadakia on the western coast of Paliki Peninsula, Cefalonia Island (Fig. 1).

### 5.1 *Sedimentary evidence*

We studied a sequence of well cemented gravel, sand and shell debris, up to 3.0 m thick, on the southern flank of Langadakia beach which is unique for the western coast of Cefalonia Island (N 38°10'33.700", E 20°21'5.100", Fig. 12). The Langadakia deposit measures around 25 m in SSW-NNE direction and 15 m in SE-NW direction. Its overall structure is well laminated with seaward, i.e. SW/SSW-dipping inclination of the strata ranging between 5° and 8° on average, strongly depending on the local topography. The length axis of the deposit corresponds well with the SSW-NNE trending lower course of the narrow Langadakia valley ending at Langadakia beach. However, towards the northeast, the conglomeratic and arenitic sequence is partly stuck to a pre-existing cliff-type rim. Highest gravel deposits belonging to the Langadakia sequence were found at 3.80 m a.s.l. (Figs. 12a and 12f).

The base of the Langadakia sequence is characterized by a clear erosional discontinuity formed in Eocene limestone. The formation of the erosional surface was obviously related to the destruction of pre-existing rock pools as fragments of rock pool rims, up to 50 cm large, were found incorporated in the lowermost coarse-grained gravel stratum (Fig. 12g). These rock pool fragments represent rip-up clasts *sensu stricto*. The Langadakia deposit consists of several fining upward sequences each of them starting with a layer of gravel up to 10–15 cm, in some cases even up to 30 cm in diameter. The grain size is clearly decreasing towards the top of each sequence to minimum coarse sand. At least four different fining upward sequences can be detected (Fig. 12a). The lowermost section of the deposit, however, is characterized by a bi- to multi-modal distribution with grain sizes ranging from 2 mm up to 50 cm (Fig. 12e). This clearly unsorted mixture seems to reflect turbulent flow dynamics. In contrast, higher units of the lowermost fining upward sequence show a fairly good degree in sorting and a clearly laminated structure indicating predominant laminar flow. In general, the degree in sorting and lamination increases towards the top of every fining upward sequence. Finer-grained sandy sections of the Langadakia deposit were intensely quarried to produce millstones, most probably for olive oil production (Fig. 12h).

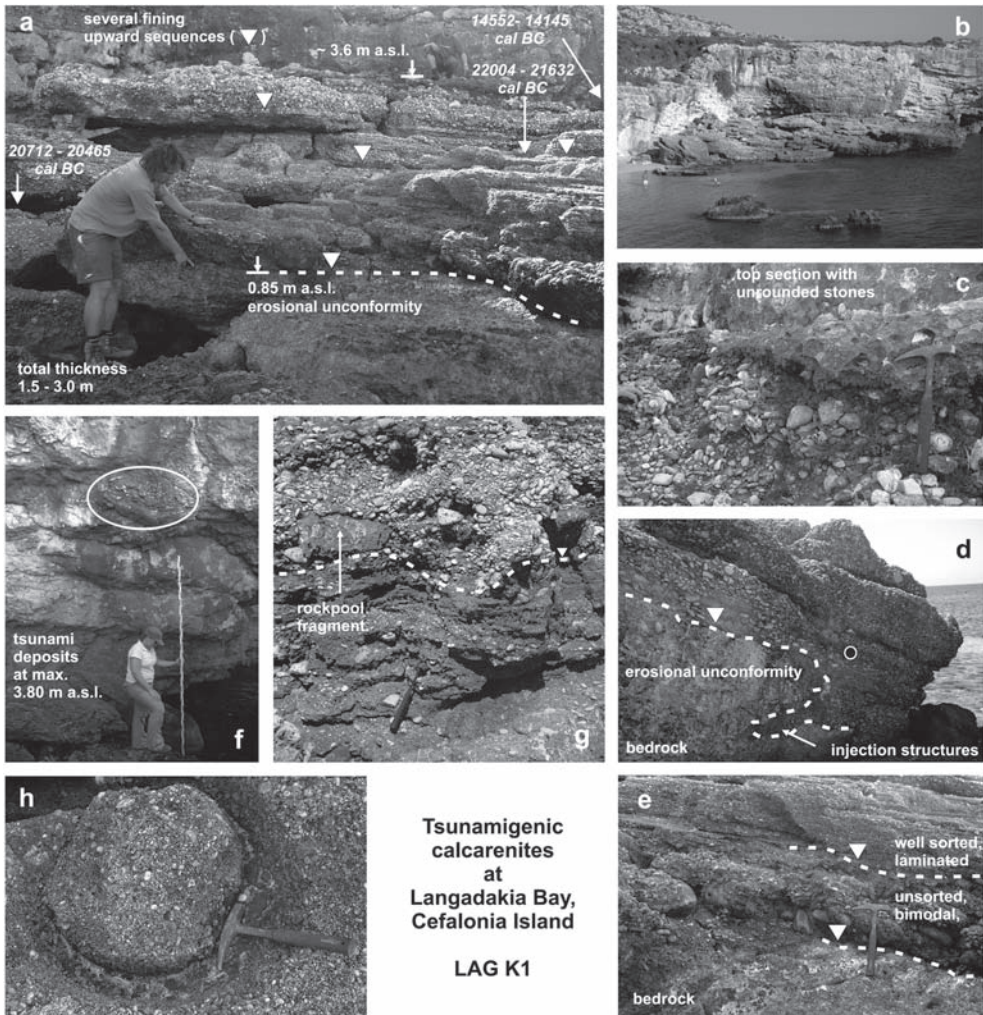


Fig. 12. The conglomeratic tsunamite encountered in the Bay of Langadakia (Cefalonia Island). (a) View of the central section of the tsunamigenic deposit with basal unconformity and several fining upward sequences. The given calibrated radiocarbon ages are pure maximum ages due to reworking effects. See Table 1 and text for further explanations; (b) general view of the conglomeratic high-energy deposit at Langadakia beach. The general SW/SSW inclination of the tsunamite layers is 5–8° and corresponds to the SSW-NNE trending narrow lower course of the Langadakia valley opening to the left of the photo; (c) top section of the Langadakia deposit including numerous angular, terrigenous stones embedded in a dense carbonate matrix; (d) injection of coarse-grained bi- to multi-modal basal deposits into a pre-existing cavity of the bedrock; diameter of lens cap (white circle) is ca. 7 cm; (e) transition from bi- or multi-modal basal deposits to well laminated fining upward sequences with an upward increase in sorting; (f) maximum elevation of tsunamigenic gravel, sand and shell debris attached to the cliff-type rim at the northeastern fringe of the Langadakia deposit; (g) basal section of tsunamite including a rock pool fragment ripped up from the underlying bedrock, on top of an erosional unconformity; (h) traces of quarrying sandy sections of the Langadakia sequence for the production of millstones. Photos taken by A. Vött, 2007, 2008.

Injection structures were found in higher parts of the Langadakia deposit where gravelly to sandy sediments had been pressed into pre-existing cavities and cracks within the bedrock (Fig. 12d). Further, we observed an overall landward thinning from around 3.0 m along the coast to around 1.50 m at the landward side of the sequence. The top section of the Langadakia deposit consists of a cemented carbonate matrix into which abundant angular stones, up to 20 cm large, are incorporated. The latter are of terrigenous origin, and presumably represent reworked alluvial fan deposits; the general appearance is the one of a strongly karstified breccia (Fig. 12c).

### 5.2 Evidence from thin section analysis

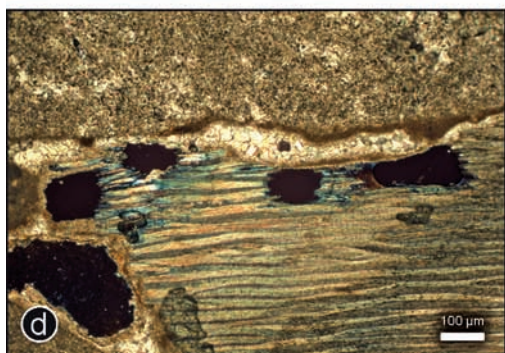
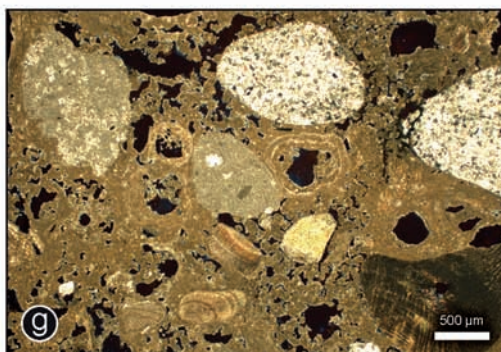
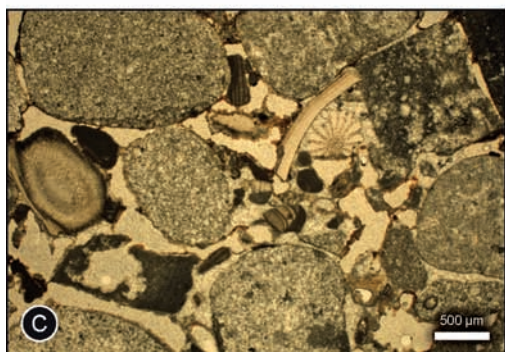
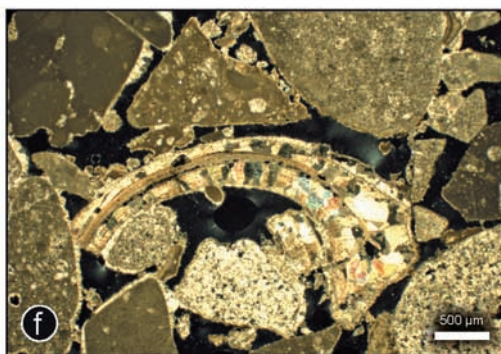
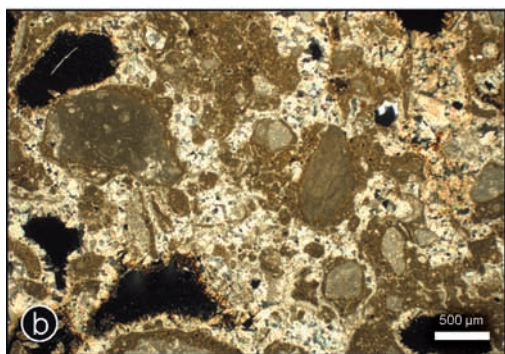
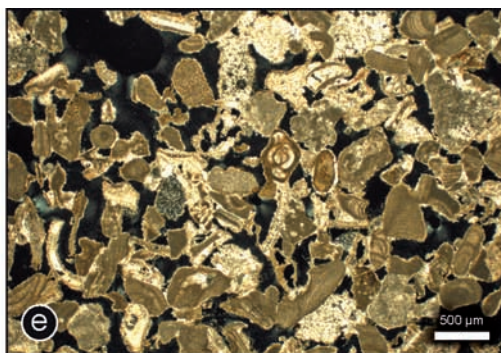
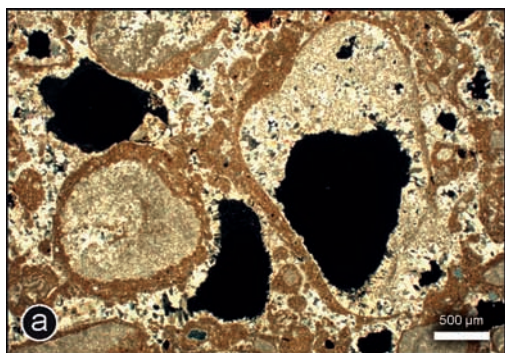
Based on thin section analyses (Fig. 13) we found that the basal part of the unit Langadakia shows a mixture of abundant shell debris, fragments of coralline algae and well rounded mineral components testifying to a marine origin of the material (Figs. 13g and 13h). A thin section from a fine gravel layer further upward also revealed abundant foraminifers, shell and algal fragments (Figs. 13e and 13f). However, angular mineral grains document that also non-littoral material was incorporated (Fig. 13f, upper center). This can also be observed for a unit of coarse gravel (Fig. 13c, upper right); still, echinoid spine fragments also reflect influence from the seaside. Microscopically, the uppermost section of the Langadakia deposit shows (sub-)angular mineral grains in a dense carbonate matrix (Figs. 13a and 13b). Large pores reflect strong dissolution and karstification followed by oxidation (Fig. 13a). In general, dissolution effects can be observed throughout the entire Langadakia sequence, affecting both carbonate matrix and shell components (Fig. 13d), with an overall increasing trend towards the top. In some places, especially in the mid-sections of the sequence, mineral and shell components show only thin coatings of carbonate cement so that the general structure is strictly component-supported (Figs. 13c, 13e and 13f).

### 5.3 Associated dislocated boulders

Geomorphological surveys conducted between Cape Gerogombos (N 38°10'42.240", E 20°20'27.670") and Cape Schinou (N 38°10'10.470", E 20°21'34.660") revealed numerous boulders up to 6–8 m a.s.l., partly in cliff top positions (Figs. 1 and 14). The boulders, partly forming imbrication trains, are characterized by bio-erosion features such as rock pools typical of the littoral zone. However, numerous boulders show rock pools facing downwards thus documenting high-energy dislocation, tilting and/or rotation.

---

Fig. 13. Thin sections of conglomeratic and calcarenitic tsunamites from the Bay of Langadakia. See Figs. 1 and 2 for locations of sampling sites, Fig. 12 for approximate stratigraphic positions of thin sections, and text for further explanations. PPL – plain polarized light, +N – crossed Nichols. (a) and (b) LAG K1 BR4 (3.27 m a.s.l.), PPL; (c) LAG K1 BR3 (2.20 m a.s.l.), PPL; (d) LAG K1 BR3 (2.20 m a.s.l.), +N; (e) LAG K1 BR2 (1.50 m a.s.l.), PPL; (f) LAG K1 BR2 (1.50 m a.s.l.), +N; (g) and (h) LAG K1 BR1 (1.35 m a.s.l.), PPL.



At Cape Gerogombos, the maximum size of dislocated boulders is around 4–6 m<sup>3</sup> (Fig. 14d), at Cape Schinou up to 8–10 m<sup>3</sup> (Figs. 14a and 14b). Additionally, we found ridges out of limestone rubble around Cape Gerogombos up to 15–20 m a.s.l. These ridges are dozens of meters long and up to 1–2 m thick consisting of blocks and stones up to 1 m in diameter.

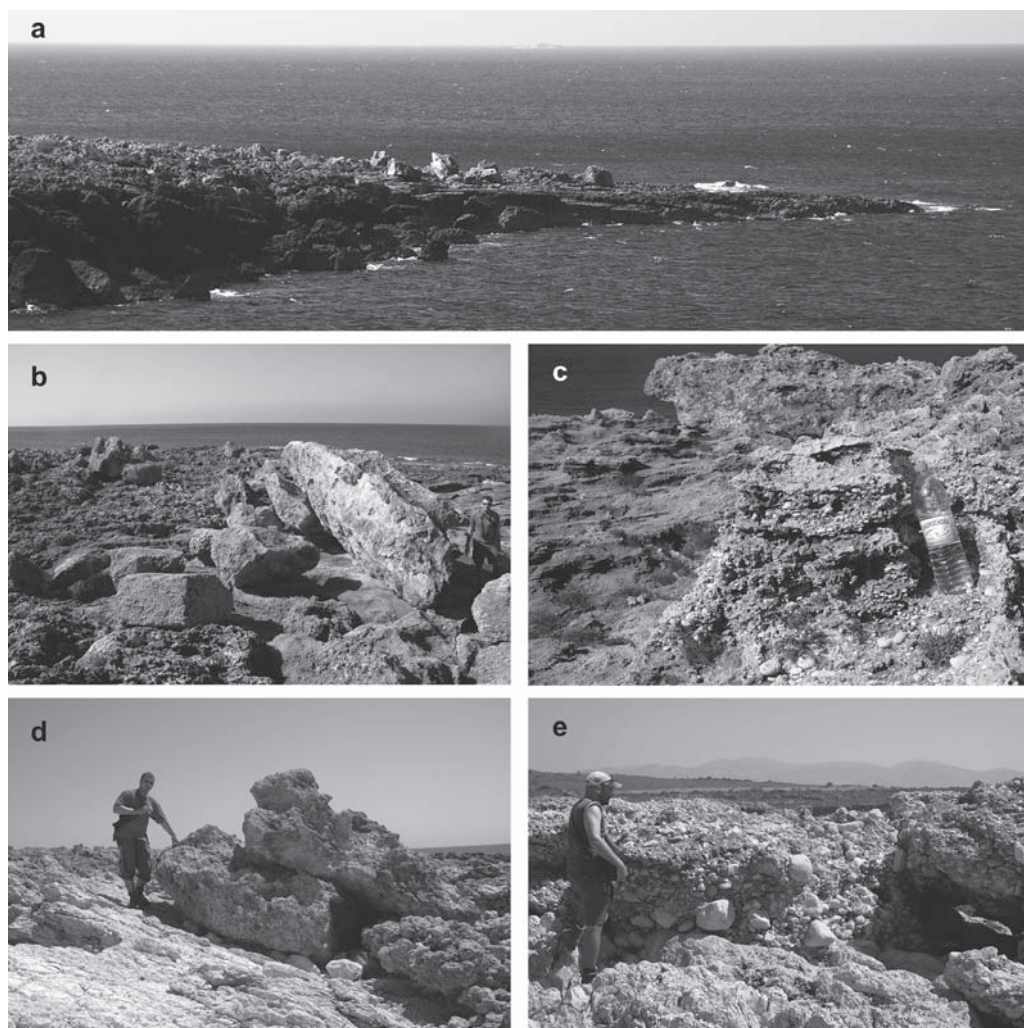


Fig. 14. Tsunami deposits encountered at Cape Schinou and Cape Gerogombos on the western coast of the Paliki Peninsula (Cefalonia Island); (a) boulders at Cape Schinou, found up to 50 m inland and up to 10 m<sup>3</sup> large, dislocated and partly imbricated by high-energy wave impact (b) and associated to conglomeratic to calcarenitic high-energy deposits showing fining upward sequences similar to the Langadakia unit (c); the dislocated boulder in the background of (c) lies in cliff top position at around 6 m a.s.l.; imbricated boulders at Cape Gerogombos (d) were also found related to cliff top high-energy conglomerates (e). Photos taken by A. Vött, 2007, 2008.

In some places, cliff top dislocated mega clasts are directly associated to conglomeratic sequences similar to the Langadakia deposit described in Section 5.1. The basal sections of these sequences, where encountered close to the sharp unconformity in the underlying bedrock, show a bi- to multi-modal grain size distribution and include gravel up to 30–40 cm in diameter (Fig. 14e). Higher sections are characterized by well laminated and fining upward sequences (Fig. 14c). The overall thickness of these cliff top conglomerates hardly exceeds 1 m (Figs. 14c and 14e) thus being considerably thinner than the maximum thickness found for the Langadakia sequence.

#### 5.4 Discussion and radiocarbon dating approach

In a summary view, the Langadakia deposit revealed geomorphological and sedimentary characteristics such as (i) a clear erosional discontinuity in the underlying bedrock, (ii) a basal multi-modal deposit including rip-up clasts, (iii) multiple fining upward sequences (graded bedding) with each sequence showing an upward increase in sorting and parallel lamination, (iv) thinning landward, and (v) associated dislocated boulders partly in cliff top position. Most of them are features empirically found typical of tsunami deposits (GOFF et al. 2001, DOMINEY-HOWES et al. 2006, KORTEKAAS & DAWSON 2007, DAWSON & STEWART 2007, MORTON et al. 2007). Considering the effects of storms on the western Paliki coast, we found drift lines out of empty plastic bottles, barrels, tires, and wooden trunk pieces accumulated by winter storms up to 8 m a.s.l. We assume maximum  $1 \text{ g/cm}^3$  as estimated density for the drifted material whereas density measurements in the laboratory yielded  $2\text{--}2.5 \text{ g/cm}^3$  for the nearby encountered dislocated boulders. Taking into account the considerable difference in volume, these data result in maximum weights of maximum few hundreds of kilograms for drifted material and 15–25 tons for dislocated boulders (maximum volume  $6\text{--}10 \text{ m}^3$ ), no matter if the movement itself happened by simple floating or by high-energy dislocation. It may therefore be excluded that boulder dislocation was caused by storm wave action.

The Langadakia sequence is interpreted as tsunami deposit which became subject to post-sedimentary cementation. Unlike in the Bay of Aghios Nikolaos case study, however, no field evidence was found how cementation had taken place. Relicts of soil covers were not encountered. In terms of event stratigraphy, it is suggested that the lowermost section of the Langadakia deposit represents turbulent flow during the first runoff of tsunami waters. Every one of the following multiple fining upward sequences is interpreted – on the base of sedimentary characteristics found for the 2004 Indian Ocean and other subrecent or historical tsunamis (NISHIMURA & MIYAJI 1995, SATO et al. 1995, SHI et al. 1995, BONDEVIK et al. 1998, HINDSON & ANDRADE 1999, FUJIWARA et al. 2000, GELFENBAUM & JAFFE 2003, MOORE et al. 2006, RICHMOND et al. 2006, BECKER-HEIDMANN et al. 2007, CHOOWONG et al. 2007, HAWKES et al. 2007, PARIS et al. 2007) – as documenting an individual tsunami wave passage across Langadakia beach. The topmost section documents increased input of terrigenous material most probably corresponding to the final backwash that induced subsequent rockfall and rapid colluvial-type accumulation of terrestrial deposits on top of a water- and carbonate-saturated event layer.

Like in the Bay of Aghios Nikolaos case study, the calcarenitic Langadakia conglomerate and sandstone meets any demands given for beachrock (Section 4.5.). Our results show that this beachrock is a distinct tsunamite reflecting strong tsunami landfall on the western coast of Cefalonia Island.

Three radiocarbon dates of marine shell fragments from the Langadakia conglomerate and sandstone rendered around 22000 cal BC (LAG K 1/5 RC, 2.60 m a.s.l.), 20500 cal BC (LAG K 1/3 RC, 1.25 m a.s.l.) and 14000 cal BC (LAG K 1/6 RC, 1.75 m a.s.l., Fig. 12, Table 1). X-ray diffractometric analyses of the samples yielded around 99 % aragonite (Fig. 15). Thus, major recrystallisation of the fossil carbonate which may have altering effects on the  $^{14}\text{C}$  age analysis (CHAPPELL & POLLACK 1972, YIM et al. 1990, BEZERRA et al. 2000, REIMER et al. 2006: 857) can be excluded. Taking into account that none of the radiocarbon ages lies close to the age determination limit of around 40000–50000 conv.  $^{14}\text{C}$  BP, the given ages are to be considered as reliable; erroneous measurement and dating can also be excluded. As the Langadakia tsunamite is suggested to contain a lot of reworked older material and fossils, age inversions were expected. They are, however, not relevant within a set of maximum ages; within an event layer out of (partly) reworked material, the youngest maximum age obtained represents the best-fit *terminus ad* or *post quem* for the formation of the deposit. We thus consider the age of 14000 cal BC as maximum age of the event.

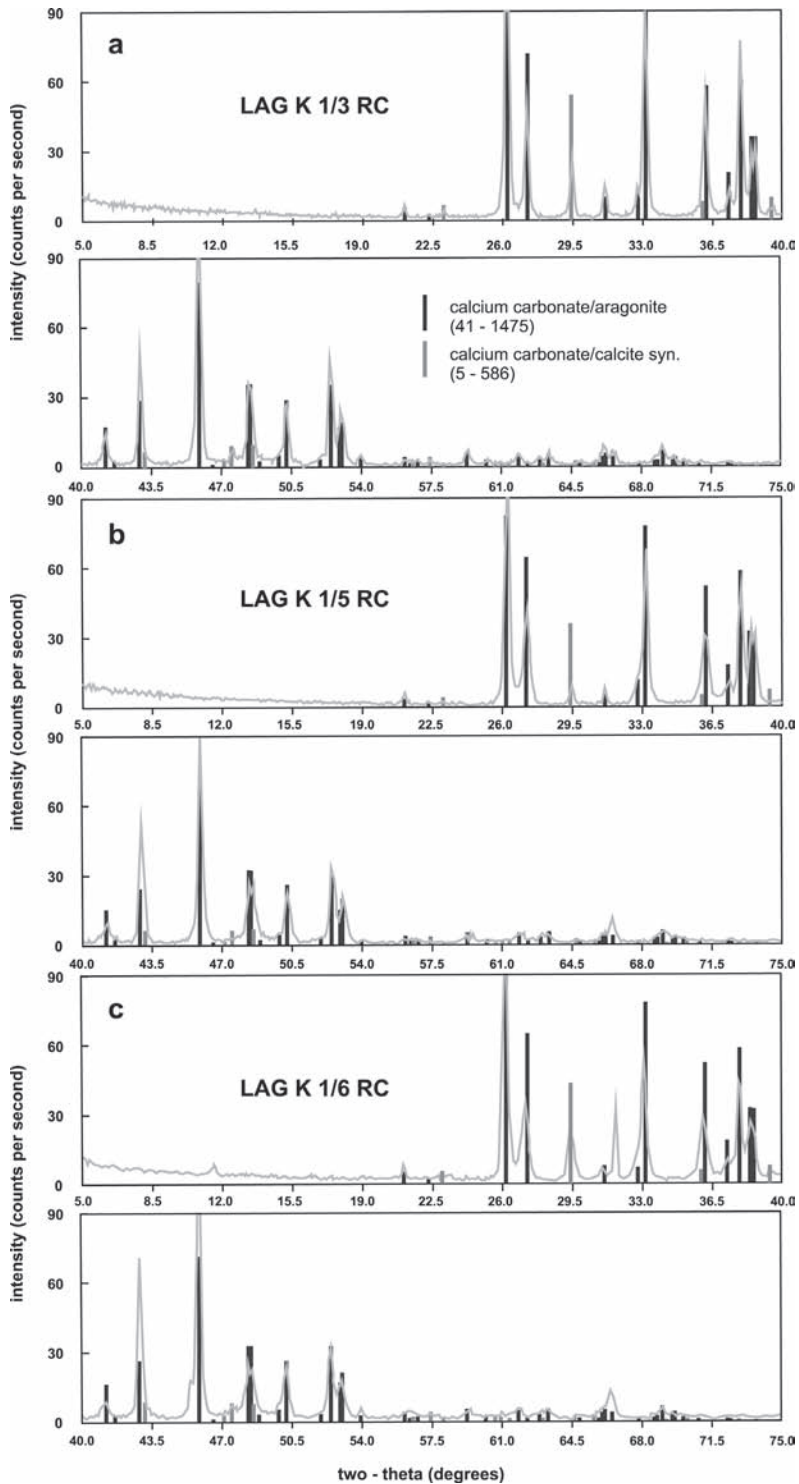
Our results offer the following scenarios. If the true age of the sequence was around 14000 cal BC, i.e. the dating result marked a *terminus ad quem*, the low palaeo sea level stand at that time would imply a tremendous tsunami runup of at least 70–80 m. This scenario seems fairly improbable as such runup heights have never been reported from the Mediterranean. We thus prefer the second scenario that the true age of the Langadakia sequence is younger, possibly even Holocene. In both cases, however, the most important result is that the Langadakia palaeotsunami deposits may not be attributed to the MIS 5 interglacial sea level highstand but have to be considered as younger, eventually Holocene lithified tsunami deposits.

## 6 Beachrock-type tsunamites in the Bay of Aghios Andreas (Peloponnese)

The Bay of Aghios Andreas is located at the northwestern end of the Katakolo Promontory some 11 km to the west of the city of Pyrgos (N 37°39'52.160", E 21°18'34.100", Fig. 1). In contrast to the long sandy shores of the adjacent Gulf of Kyparissia, the coast, exposed towards the west, is characterized by numerous indentations, rocky cliffs and small islands lying not far offshore. The coastal setting thus reflects disturbance and strong erosion and is far away from having reached a state of geomorphodynamic equilibrium. The archaeologi-

---

Fig. 15. X-ray diffractograms for radiocarbon dated samples LAG K 1/3 RC, LAG K 1/5 RC and LAG K 1/6 RC taken from the Langadakia tsunamite showing that major recrystallisation of the fossil aragonitic carbonate can be excluded. The ages obtained are thus to be considered as reliable. See text for further explanations.



cal remains of Pheia – the harbour of ancient Olympia (STRABO 8, 2, 13, see GROSKURD 1831) – were found lying partly onshore, partly underwater in the Bay of Aghios Andreas. The ancient landing place is reported to have been destroyed and sunk underwater by an earthquake in the 6<sup>th</sup> century AD (KRAFT et al. 2005). Our studies in the Bay of Aghios Andreas included geomorphological and sedimentological surveys, GPS and LIDAR measurements, sampling for thin section analyses, and vibracoring. Special focus was laid on local beachrock deposits for which the bay is well known and which were subject to previous studies (e.g. FOUACHE & DALONGEVILLE 1998).

### 6.1 *Sedimentary evidence*

In the Bay of Aghios Andreas, beachrock can be observed along the present shore from present mean sea level up to 1.50 m a.s.l. where it disappears towards inland under younger soil material (Figs. 16 and 17). Towards the sea, lower beachrock sections can be found several dozens of meter offshore in shallow water depths. The thickness of the beachrock varies along the beach with a maximum value in the central section of the bay and getting thinner towards the north and south.

By our geomorphological and sedimentological studies, the following characteristics of the beachrock were encountered: (i) In the southern part of the bay, the beachrock partly lies on top of an erosional unconformity formed in grey Neogene marls and siltstones (Fig. 17a). (ii) The basal section of the beachrock, some 20–30 cm thick, is largely dominated by gravel, up to 15 cm in diameter. It is followed by a thick stratum of mean to fine sand, clearly laminated, and consisting of several fining upward sequences with local intercalations of coarse sand and marine shell debris (Figs. 17b and 17c). (iii) Locally, the well laminated mid-section with its fining upward sequences is covered by a fairly unsorted gravelly to sandy top section including ceramic fragments (Fig. 17a). (iv) The overall inclination of the beachrock strata is 6–8°. (v) The sandy beachrock unit is covered by a homogeneous layer of beige-coloured silt to fine sand which seems to be of aeolian nature.

We found ashlar, up to 50 x 30 x 20 cm<sup>3</sup> large, incorporated into the sandy mid-section of the beachrock (Figs. 16b and 16d). The ashlar are still angular, in places even with remains of white plaster adhering to their surface. This indicates that they were not subject to littoral processes (Fig. 16b). Additionally, numerous ceramic fragments were encountered both in the laminar mid-section and in the unsorted top section of the beachrock, almost all of them sharply edged (Fig. 17a).

Further sedimentary features, outstandingly untypical of a littoral environment, were found. First, numerous beachrock sections show load cast structures, especially below large intra-clasts such as ashlar (Fig. 16d) and large pieces of gravel and stones (Fig. 17a). Second, extensive convolute bedding appears in the upper mid-section of the beachrock sequence (Fig. 17e). Both findings indicate rapid sediment deformation shortly after deposition when the accumulated sands were still saturated by water and thus unstable. Convolute bedding documents slump and/or avalanche-like downward movement of paste- or sus-

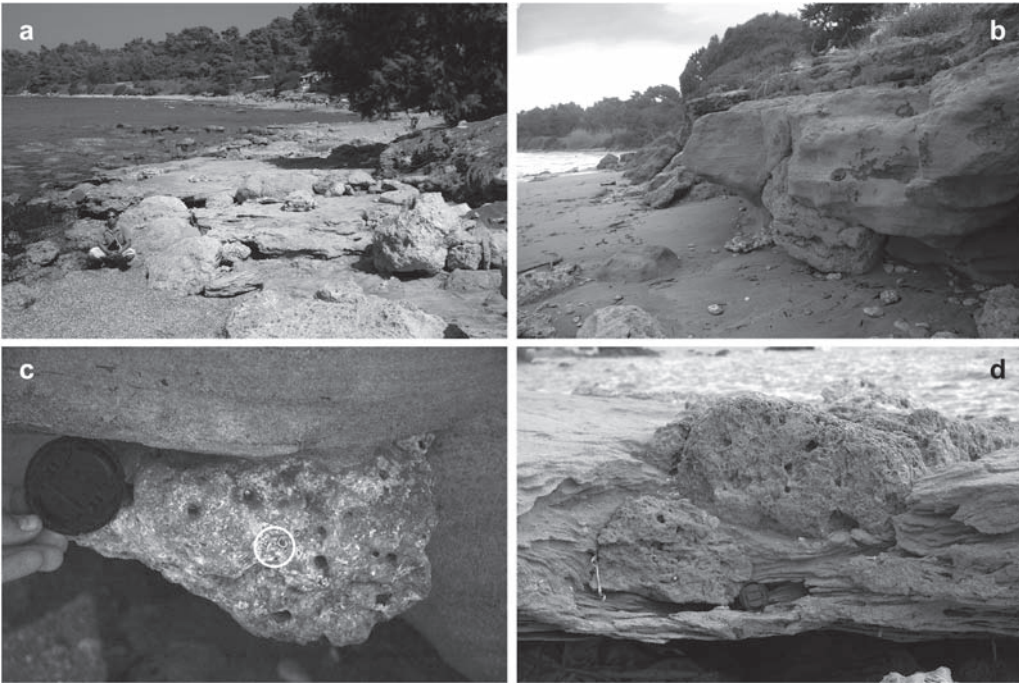


Fig. 16. View of the Bay of Aghios Andreas near Pyrgos (Peloponnese) where Pheia, the ancient harbour of Olympia, is located (Strabo 8, 3, 12, see GROSKURD 1831). The site is well known for the occurrence of beachrock, up to 3 m thick and reaching up to 2.60 m a.s.l. (a); the mid-section of the beachrock is made out of well laminated cemented sand with several fining upward sequences locally showing enclosed large intra-clasts such as angular ashlar with in-situ remains of white plaster (b) or stones with bio-erosion features from the littoral zone such as boreholes and in-situ boring organisms (c); diameter of lens cap is ca. 7 cm; incorporation of ashlar partly induced load cast features (d); sedimentary characteristics of the beachrock cannot be explained by usual littoral processes but rather reflect high-energy impact and flooding of the site. Vibracore AND 6, drilled 40 m inland, revealed a destruction layer underneath the beach-rock type calcarenitic tsunamite including ceramic fragments. Geoarchaeological and sedimentary findings thus document tsunamigenic destruction of Olympia's ancient harbour by a probably earthquake-related tsunami in the 6<sup>th</sup> cent. AD. Photos taken by A. Vött, 2008, 2009.

pension-like sediments (FÜCHTBAUER 1988). Numerous marine shell fragments as well as incorporated blocks, up to 30 cm large and characterized by boreholes and in-situ specimens of boring organisms, prove that the sedimentary impulse came from the seaside (Fig. 16c, Fig. 17b).

Vibracore AND 6 (N 37°39'55.620", E 21°18'36.238", ground surface 8.09 m a.s.l.) was drilled some 40 m inland. In this core, we encountered sandy beachrock sandy deposits between 2.60 m a.s.l. and 0.53 m b.s.l. with a total thickness of around 3 m. These findings clearly indicate a landward increase in elevation of the beachrock strata. At the immediate base of the AND 6 beachrock, a debris layer was found including ceramic fragments associ-

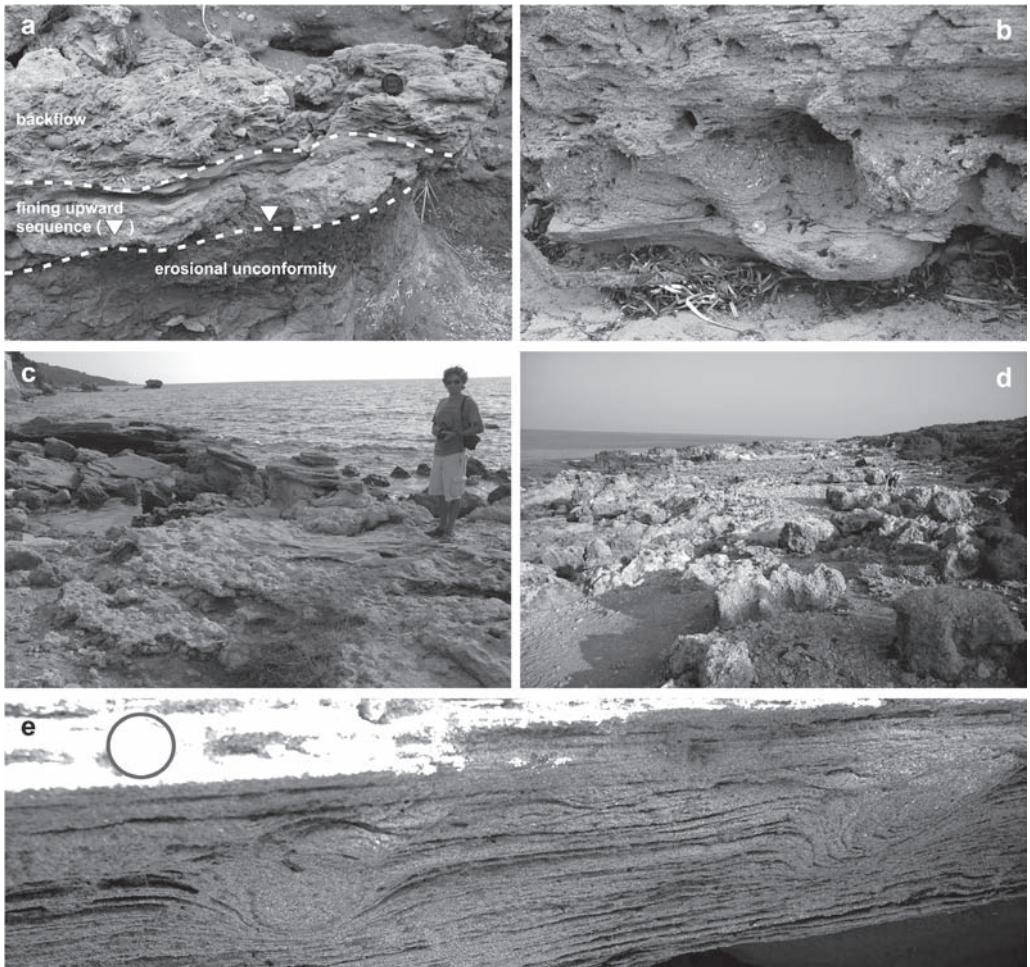


Fig. 17. Selected sedimentary characteristics of the beachrock-type calcarenitic tsunamite at Aghios Andreas and geomorphological traces of high-energy wave impact on the coast; (a) sharp erosional unconformity encountered at ca. 1.20 m a.s.l. in the southern part of the bay formed in Neogene marls and siltstones. The discontinuity is covered by a fining upward sequence of cemented sand and subsequent bi- to multi-modal backflow deposits, partly gravity driven, with abundant angular stones of terrigenous origin and ceramic fragments; (b) mid-section of beachrock characterized by several fining upward sequences locally starting with layers of coarse sand and shell debris; (c) basal section of beachrock-type tsunamite made out of gravel, up to 15 cm large, cemented in a sandy matrix, on top of an erosional discordance; (d) dislocated boulders found up to 40–80 m distant from the coast at the Katakolo Promontory and near Aghios Andreas beach associated to beachrock-type tsunamites; (e) detail of the upper mid-section of the Aghios Andreas beachrock showing convolute bedding in a fining upward sequence; the black circle is a 2 Euro coin. Convolute bedding is completely untypical of forming processes in a non-tidal littoral zone. It indicates gravity-induced flow dynamics in a water-saturated suspension-like matrix; here, convolute bedding structures reflect intermittent backflow shortly after high-energy deposition of thick allochthonous sand deposits onshore. Photos taken by A. Vött, 2008, 2009.

ated to a silty to clayey sediment. This quiescent water deposit seems to reflect the original sedimentary environment of the ancient harbour prior to its destruction.

Based on geo-scientific evidence, the following conclusions can be made. (i) The Aghios Andreas beachrock unit shows numerous sedimentary characteristics typical of high-energy influence, such as an erosional unconformity, intra- and rip-up clasts, multi-modal and chaotically structured sediment layers, and fining upward sequences. (ii) Signs of load casting and convolute bedding are characteristic for weight-induced non-littoral gravity flows in water-saturated deposits shortly after sediment deposition. (iii) Numerous geoarchaeological traces indicate rapid incorporation of ashlar and ceramic fragments into the sediment without destroying sharp ashlar angles or even plaster.

The Aghios Andreas beachrock thus must not be considered as consolidated littoral sediment but rather as a cemented high-energy event deposit. Our interpretation is based on sedimentary characteristics found typical of tsunami influence all over the world and mentioned in Section 5.4. From a sedimentological point of view, the basal section of the beachrock is interpreted as runup deposit accumulated under turbulent conditions whereas the thick and well laminated mid-section with its multiple fining upward sequences seems to reflect predominant laminar flow and the multiple passage of tsunami waves. In some places, chaotically structured and coarse-grained backwash deposits were subsequently accumulated; in other places, where turbulent backwash did not occur, water-saturated tsunami sands partially flowed back and produced convolute bedding. This was possibly triggered by seismic aftershocks. Because of the aeolian-type silty to fine sandy cover of the beachrock we suggest that, after the deposition of the event sequence, coastal winds have blown out finer grain sizes and formed coastal dunes on top of more landward parts of the tsunami deposits. Post-sedimentary cementation of the tsunamigenic and aeolian units are assumed to have taken place under subaerial conditions, most probably under a soil cover, similar to the Aghios Nikolaos situation (see Section 4.4).

Further evidence of tsunami influence is given by numerous dislocated boulders, up to 2–8 m<sup>3</sup> large, which we found lying up to 40–80 m inland along the Bay of Aghios Andreas and the Katakolo Promontory (Fig. 17d).

## 6.2 Discussion and geoarchaeological dating

Numerous ceramic fragments and several angular ashlar encountered within and directly beneath the beachrock-type calcarenite in the Bay of Aghios Andreas prove a Holocene age of the deposit. Older studies dating the “Littoral limestone of Ayios Andreas” to the Pleistocene epoch (IGMR 1980) have therefore to be considered incorrect. YALOURIS (1957, 1960) found abundant archaeological remains proving human occupation of the Pheia area for most periods from Early Helladic through Roman to Byzantine times. Sherds from different cultural epochs were encountered in similar stratigraphic positions on land, underwater and cemented within the beachrock. Additionally, remains of buildings were found underwater up to a distance of 200 m from the shore and down to 5 m water depth. The youngest archaeological findings were dated to the 6<sup>th</sup> cent. AD (YALOURIS 1957, 1960).

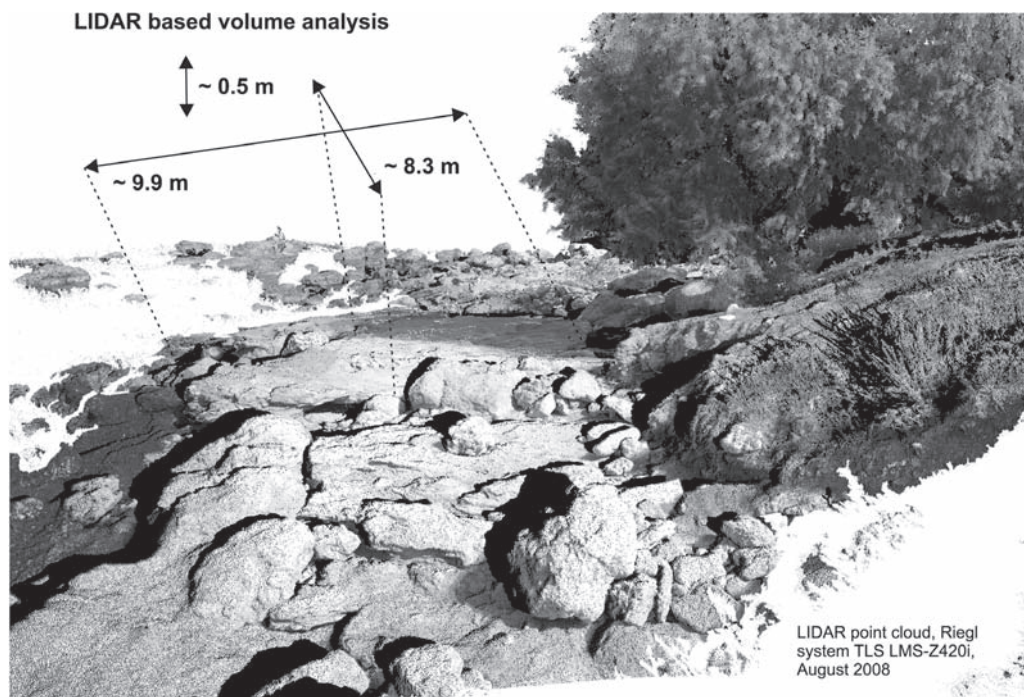


Fig. 18. 3D-visualisation of beachrock-type tsunamites at Aghios Andreas based on high-resolution LIDAR measurements accomplished with a Riegl TLS LMS-Z420i instrument with an average accuracy of 6 mm; the LIDAR point cloud is combined with digital photographic data. The coherent beachrock-section in the center represents a volume of around 13 m<sup>3</sup> of allochthonous tsunami deposits. It can be clearly seen how the beachrock surface disappears under a cover of younger, mostly colluvial deposits (right center). DGPS data show that the maximum elevation of the exposed beachrock is 1.50 m a.s.l.; vibracorings further inland revealed the same stratigraphic unit up to 2.60 m a.s.l. The beachrock-type calcarenite at Aghios Andreas beach represents part of a tsunamite uncovered by littoral erosion processes.

Based on literature studies, KRAFT et al. (2005) reconstructed the palaeogeography of the Bay of Aghios Andreas, assuming that ancient Pheia was destroyed by an earthquake and sunk into the sea by co-seismic subsidence of the harbour area and coincidental uplift of the Katakolo ridge. However, our geomorphological studies in the Katakolo area did not reveal any evidence of young coastal uplift such as uplifted marine notches or uplifted abrasion platforms. FOUACHE & DALONGEVILLE (1998, 2004) suggest that Pheia had already been subject to gradual coastal subsidence of about 6.5 m between Classical and Byzantine times before it experienced destructive earthquakes in 521 and/or 551 AD. The beachrock, according to their opinion, formed out of littoral deposits after a subsequent 1.5 m uplift in the 6<sup>th</sup> cent. AD (FOUACHE & DALONGEVILLE 2004). Well dated relative sea level curves for the northwestern, western and southwestern Peloponnese published by KRAFT et al. (2005), VÖTT (2007), and ENGEL et al. (2009), however, show a more or less constantly

rising sea level with rates between 0.5–0.7 m/ka; one major result of these studies is that the relative sea level has never been higher than at present. Moreover, HOLLENSTEIN et al. (2008b), based on continuous DGPS measurements, report on co-seismic vertical crustal movements for the Peloponnese area within the range of maximum 1–2 decimeters. Against this background, the assumptions of FOUACHE & DALONGEVILLE (1998) – 6.5 m of gradual subsidence for the ca. 1000-year-long period between Classical and Byzantine times, for which archaeological remains document the proper use of Pheia as Olympia's harbour, and 1.5 m of subsequent co-seismic uplift – are not realistic; this is especially true if seen together with yo-yo effects for which no corresponding on- and/or offshore deposits or any geomorphological evidence were found. Although the Aghios Andreas beachrock sequence and its peculiar allochthonous contents were described in detail by KRAFT et al. (2005) and FOUACHE & DALONGEVILLE (1998, 2004), both groups of authors did not give any explanations how this kind of sediment was formed.

As shown by our study, the Aghios Andreas beachrock material cannot be explained as usual littoral deposit. Geomorphological, geoarchaeological and sedimentary findings rather revealed that it is a cemented tsunamite. We suggest that, by tsunami landfall, large parts of the coast were eroded and tsunami sediments were deposited along the shore incorporating cultural debris. Where deposited in or below sea level, tsunami deposits were reworked and redistributed; where deposited above mean sea level, cementation and conservation of the tsunamigenic material took place, most probably under a soil cover. Final tsunamigenic destruction of Pheia can be dated to the 6<sup>th</sup> cent. AD according to the youngest artifacts enclosed in the tsunamigenic beachrock and considering continuous human presence since the Early Helladic (*terminus ad quem*, see Section 6.1). We further suggest that this tsunami was associated to one of the major earthquakes known from the 6<sup>th</sup> cent. AD (in the years 521 AD and 551 AD) that were primarily thought responsible for Pheia's destruction (YALOURIS 1957, FOUACHE & DALONGEVILLE 1998, KRAFT et al. 2005). Analogous to the 1999 Izmit earthquake and tsunami in western Turkey (ALTINOK et al. 2001), it may be assumed that co-seismic subsidence occurred and aggravated the destruction of the site. The Aghios Andreas beachrock thus represents a calcarenitic tsunamite testifying to the event-related destruction of ancient Olympia's harbour in the 6<sup>th</sup> cent. AD.

## 7 General discussion

In this paper, we present results from three case studies on calcarenitic tsunamites encountered in three different coastal environments in western Greece. In either case, the described tsunamite is in accordance with the scientific definition of beachrock *sensu stricto* as hard coastal sedimentary formation out of beach material rapidly cemented by calcitic or aragonitic carbonate precipitation (e.g. BRICKER 1971, SHORT 2005, TURNER 2005, VOUSDOKAS et al. 2007, BIRD 2008, see discussion in Sections 4.5, 5.4 and 6.2). The Aghios Andreas case study was even subject to several beachrock studies (FOUACHE & DALONGEVILLE 1998, 2004 and literature therein). Our results thus infer some general questions on the nature and occurrence of beachrock and on its usability for the reconstruction of palaeogeographies and past coastal processes.

Our case studies clearly document that beachrock may represent the cemented and possibly only left-over part of formerly thicker tsunami deposits. Although this paper does not intend to equalize any form of beachrock with calcarenitic tsunamites our results have to be kept in mind when beachrock is intended to be used as indicator of littoral processes or sea level evolution. The latter has been done in various geo-scientific studies all over the world, especially in order to reconstruct palaeo sea level stands. Albeit, it is still a matter of vivid discussion if beachrock as such – seen as lithified beach deposits – can be used for sea level reconstruction at all (KELLETTAT 2006, 2007, KNIGHT 2007). From our point of view, it has to be stated that using the beachrock encountered in the Bays of Aghios Nikolaos (Akarnania), Langadakia (Cefalonia) and Aghios Andreas (Peloponnese) as sea level indicators would result in a misleading and incorrect reconstruction of the local sea level history; beachrock-based palaeo sea level data would strongly contradict local relative sea level data found on the basis of reliable geoarchaeological and sedimentary indicators (e.g. RAPHAEL 1973, 1978, JING & RAPP 2003, KRAFT et al. 2005, VÖTT 2007, ENGEL et al. 2009). In every one of the presented case studies, the beachrock represents a part of a tsunamigenic sequence, subaerially deposited and cemented way above the sea level at the time of deposition. Actually, it is a matter of accident which part of the beachrock is conserved and visible along the beach. Close to the Aghios Andreas chapel, for instance, we found the same stratigraphic beachrock unit at around 40 cm a.s.l. at the immediate waterfront, at 1.50 m a.s.l. where it disappears under soil material, and even considerably higher in vibracore AND 6 some 40 m inland, that means over considerable distances and in different elevations. Further problems arise from lateral and landward thinning of beachrock-type tsunami deposits. Based on our data, we therefore strongly recommend not using beachrock as indicator for relative sea level reconstruction unless a tsunamigenic nature of the beachrock can be excluded.

Another open question is how the cementation of beachrock *sensu stricto* takes place. One group of scientists suggest supratidal cementation in the spray zone by decreasing CO<sub>2</sub> partial pressure (KELLETTAT 1975, 1998, 1999: 163ff., 2006); another group approves cementation in the near-coast intertidal zone where carbonate-saturated marine groundwater meets fresh groundwater. The latter process is assumed to result in a sudden reduction of the maximum solubility product and subsequent carbonate precipitation (DESRUELLES et al. 2004, 2007, TURNER 2005, VOUSDOKAS et al. 2007, further references therein). The Aghios Nikolaos case study, however, revealed an alternative way of beachrock formation. Geomorphological, sedimentological and geochemical evidence suggests post-sedimentary cementation by subaerial decalcification of higher sections and encrustation of lower sections of a tsunamigenic unit by pedogenetic processes. This formation is bound to areas with considerable amounts of annual rainfall enabling a net downward percolation of soil water and associated downward transfer of temporarily dissolved compounds (Section 4.4).

## 8 Conclusions

Based on detailed geomorphological, sedimentological and geochemical investigations on calcarenitic onshore deposits in three coastal areas in western Greece, the following conclusions can be made.

(i) Near- and onshore calcarenitic and conglomeratic deposits encountered in the Bays of Aghios Nikolaos (Akarnania), Langadakia (Cefalonia Island) and Aghios Andreas (Peloponnese) are identified as cemented high-energy tsunami deposits. Due to their allochthonous character, they cannot be explained by current littoral processes. We found sedimentary characteristics such as basal erosional unconformities, rip-up clasts, large intra-clasts, multiple fining upward sequences showing an upward increase in sorting and clear lamination as well as bi- to multi-modal grain size distribution all of which are reported as typical of tsunami deposits.

(ii) Further sedimentary features reflecting non-littoral but rather high-energy impact are injection structures, load casts and convolute bedding. In some cases, tsunami layers were found associated to dislocated boulders.

(iii) Thin section analyses revealed that the calcarenitic tsunamites predominantly consist of material from marine to littoral environments. Findings of angular to sharply edged mineral grains, partly coated with oxides or covered by pyrite, however, show that sediments from terrestrial or quiescent water anoxic environments were also incorporated. This is due to large scale tsunami inundation affecting both shore and surrounding areas.

(iv) Micromorphological studies of calcarenitic tsunamites brought to light traces of high pressure shock destruction of mineral grains and bedrock fragments such as the formation of sharply edged flakes by impacting, cracking and shearing effects. Our data indicate that, in some cases, the deposits, once accumulated by an impact, were not moved or altered by littoral or other major processes before subsequent cementation took place.

(v) Tsunami deposits presented in this paper are generally characterized by a threefold structure. The base of each tsunamite is made up of bi- to multi-modal sediments including large rip-up and intra-clasts and gravel. It is suggested that this section reflects initial tsunami landfall and associated turbulent flow dynamics during runup. The subsequent set of several predominantly well laminated fining upward sequences documents the multiple passage of tsunami waves during inundation under prevailingly laminar flow conditions. Depending on the local topography, it is covered by a section of unsorted material including numerous terrigenous stones most probably revealing backwash dynamics. In the presented case studies, the well laminated mid-section shows the maximum thickness.

(vi) Where encountered at the immediate seafront, the cemented tsunamigenic calcarenites and conglomerates match the definition of beachrock *sensu stricto*. This is thus the first study that reveals the tsunamigenic nature of selected beachrock sequences in the Mediterranean.

(vii) Beachrock-type tsunamites do not, in every case, represent the entire tsunamigenic sedimentary sequence. Locally, only the lowermost section is cemented; it can be found as beachrock along the shore after non-cemented top sections have been removed by coastal erosion. In Aghios Nikolaos, post-depositional cementation took place by pedogenetic processes. Once deposited sufficiently above sea level, top sections of tsunami deposits were decalcified and dissolved carbonate transported downward by rainwater percolation. Subsequent secondary carbonate precipitation occurs where porosity abruptly decreases or in the groundwater level.

(viii) Age determination of beachrock-type tsunamites by radiocarbon dating of fossil carbonate shells or plant remains is problematic due to reworking effects and yields simple maximum ages. Using a combined approach of radiocarbon, OSL and archaeological dating, however, the obtained ages are in good accordance with local tsunami chronostratigraphies. For the Langadakia sequence, XRD measurements helped to exclude major recrystallisation and to establish a late Pleistocene or even Holocene age.

(ix) Spectacular results from geoarchaeological studies in the Bay of Aghios Andreas document that Olympia's ancient harbour site Pheia was finally destroyed by strong tsunami impact in the 6<sup>th</sup> cent. AD.

(x) Based on our findings of beachrock-type calcarenitic and conglomeratic tsunamites we strongly recommend not using beachrock as sea level indicator for the reconstruction of palaeo sea level fluctuations unless a tsunamigenic nature of the beachrock can definitely be excluded.

### *Acknowledgements*

Sincere thanks are due to A. Bonetti (Tragata), K. Gaki-Papanastassiou, H. Maroukian and D. Papanastassiou (Athens) for joint field survey. We thank U. Ewelt (Grünberg), T. Kirkos (Vonitsa), L. Kolonas (Athens), C. Melisch (Berlin), M. Stravropoulou (Mesolongion), and H. Warnecke (Rösrath) for various support during field work and fruitful discussions. We are further indebted to H. Nödler and C. Mann (Marburg) for professional cartographic services. P.M. Grootes (Kiel) accomplished radiocarbon analyses. Work permits were kindly issued by I. Zananiri and C. Perissoratis from the Greek Institute of Geology and Mineral Exploration (IGME, Athens). We thank G. Mastronuzzi (Bari) and an anonymous reviewer for valuable comments on the manuscript. Field and laboratory studies were conducted within the framework of the interdisciplinary project "Quaternary tsunami events in the eastern Ionian Sea" (2009-2012); funding by the German Research Foundation (Bonn, VO 938/3-1) is gratefully acknowledged.

### **References**

- ALTINOK, Y., TINTI, S., ALPAR, B., YALÇINCER, A.C., ERSOY, Ş., BORTOLUCCI, E. & ARMIGLIATO, A. (2001): The tsunami of August 17, 1999 in Izmit Bay, Turkey. – *Nat. Hazards* **24**: 133–146.
- BECKER-HEIDMANN, P., REICHERTER, K. & SILVA, P.G. (2007): <sup>14</sup>C-charcoal and sediment drilling cores as first evidence of Holocene tsunamis at the southern Spanish coast. – *Radiocarbon* **49** (2): 827–835.
- BERNASCONI, M.P., MELIS, R. & STANLEY, J.-D. (2006): Benthic biofacies to interpret Holocene environmental changes and human impact in Alexandria's Easter Harbour, Egypt. – *The Holocene* **16** (8): 1163–1176.
- BEZERRA, F.H.R., VITA-FINZI, C. & FILHO, F.P.L. (2000): The use of marine shells for radiocarbon dating of coastal deposits. – *Rev. Brasil. Geoci.* **30** (1): 211–213.
- BIRD, E. (2008): *Coastal Geomorphology*. – 2<sup>nd</sup> edition, 436 pp.; Wiley, Chichester.
- BONDEVIK, S., SVENDSEN, J.I. & MANGERUD, J. (1998): Distinction between the Storegga tsunami and the Holocene marine transgression in coastal basin deposits of western Norway. – *J. Quatern. Sci.* **13** (6): 529–537.

- BRICKER, O.P. (1971): Introduction: beachrock and intertidal cement. – In: BRICKER, O.P. (ed.): Carbonate Cements. – 1–13; Johns Hopkins Press, Baltimore.
- BROADLEY, L., PLATZMAN, E., PLATT, J. & MATTHEWS, S. (2004): Palaeomagnetism and tectonic evolution of the Ionian thrust belt, NW Greece. – In: CHATZIPETROS, A. & PAVLIDES, S. (eds.): Proceedings of the 5<sup>th</sup> International Symposium on Eastern Mediterranean Geology, 14–20 April 2004, Thessaloniki, Greece. – Vol. **II**: 973–976.
- BRUINS, H.J., MACGILLIVRAY, J.A., SYNOLAKIS, C.E., BENJAMINI, C., KELLER, J., KISCH, H.J., KLÜGEL, A. & VAN DER PFLICHT, J. (2008): Geoarchaeological tsunami deposits at Palaiokastro (Crete) and the Late Minoan IA eruption of Santorini. – *J. Archaeol. Sci.* **35**: 191–212.
- BRUZZI, C. & PRONE, A. (2000): Une méthode d'identification sédimentologique des dépôts de tempête et de tsunamis: L'exoscopie des quartz, résultats préliminaires. – *Quaternaire* **11** (3–4): 167–177.
- CHAPPELL, J. & POLACH, H.A. (1972): Some effects of partial recrystallisation on <sup>14</sup>C dating late Pleistocene corals and mollusks. – *Quatern. Res.* **2**: 244–252.
- CHOOWONG, M., MURAKOSHI, N., HISADA, K., CHARUSIRI, P., DAORERK, V., CHAROENTITIRAT, T., CHUTAKOSITKANON, V., JANKAEW, K. & KANJANAPAYONT, P. (2007): Erosion and deposition by the 2004 Indian ocean tsunami in Phuket and Phang-nga Provinces, Thailand. – *J. Coastal Res.* **23** (5): 1270–1276.
- COCARD, M., KAHLE, H.-G., PETER, Y., GEIGER, A., VEIS, G., FELEKIS, S., PARADISSIS, D. & BILLIRIS, H. (1999): New constraints on the rapid crustal motion of the Aegean region: recent results inferred from GPS measurements (1993–1998) across the West Hellenic Arc, Greece. – *Earth and Planet. Sci. Lett.* **172**: 39–47.
- DAWSON, A.G. (1994) Geomorphological effects of tsunami run-up and backwash. – *Geomorphology* **10** (1–4): 83–94.
- DAWSON, A.G. & STEWART, I. (2007): Tsunami deposits in the geological record. – *Sediment. Geol.* **200**: 166–183.
- DE MARTINI, P.M., BURRATO, P., PANTOSTI, D., MARAMAI, A., GRAZIANI, L. & ABRAMSON, H. (2003): Identification of tsunami deposits and liquefaction features in the Gargano area (Italy): paleoseismological implication. – *Ann. Geophys.* **46** (5): 883–902.
- DESRUÉLLES, S., FOUACHE, E., PAVLOPOULOS, K., DALONGEVILLE, R., PEULVAST, J.-P., COQUINOT, Y. & POTDEVIN, J.-L. (2004): Beachrock and recent sea-level changes on Mykonos, Delos and Rhénia Islands (Cyclades, Greece). – *Géomorphologie: relief, processus, environnement* **1**: 5–18.
- DESRUÉLLES, S., FOUACHE, E., DALONGEVILLE, R., PAVLOPOULOS, K., PEULVAST, J.-P., COQUINOT, Y., POTDEVIN, J.-L., HASENOHR, C., BRUNET, M., MATHIEU, R. & NICOT, E. (2007): Sea-level changes and shoreline reconstruction in the ancient city of Delos (Cyclades, Greece). – *Geodynamica Acta* **20** (4): 231–239.
- DOMINEY-HOWES, D.T.M., CUNDY, A. & CROUDACE, I. (2000): High energy marine flood deposits on Astypalaea Island, Greece: possible evidence for the AD 1956 southern Aegean tsunami. – *Marine Geol.* **163**: 303–315.
- DOMINEY-HOWES, D.T.M., HUMPHREYS, G.S. & HESSE, P.P. (2006): Tsunami and palaeotsunami depositional signatures and their potential value in understanding the late-Holocene tsunami record. – *The Holocene* **16** (8): 1095–1107.
- DONATO, S.V., REINHARDT, E.G., BOYCE, J.I., ROTHBAUS, R. & VOSMER, T. (2008): Identifying tsunami deposits using bivalve shell taphonomy. – *Geology* **36** (3): 199–202.
- DOUTSOS, T. & KOKKALAS, S. (2001): Stress and deformation patterns in the Aegean region. – *J. Struct. Geol.* **23**: 455–472.
- ENGEL, M., KNIPPING, M., BRÜCKNER, H., KIDERLEN, M. & KRAFT, J.C. (2009): Reconstructing middle to late Holocene palaeogeographies of the lower Messenian plain (southwestern Peloponnese, Greece): Coastline migration, vegetation history, and sea level change. – *Palaeogeography, Palaeoclimatology, Palaeoecology* **284**: 257–270.

- FLOTH, U., VÖTT, A., MAY, S.M., BRÜCKNER, H. & BROCKMÜLLER, S. (2009): Geo-scientific evidence versus computer models of tsunami landfall in the Lefkada coastal zone (NW Greece). – In: VÖTT, A. & BRÜCKNER, H. (eds.): *Ergebnisse aktueller Küstenforschung – Beiträge zur 26. Jahrestagung des Arbeitskreises Geographie der Meere und Küsten*, 25.–27. April 2008, Marburg an der Lahn. – *Marburger Geographische Schriften* **145**: 140–156.
- FOUACHE, E. & DALONGEVILLE, R. (1998). Neotectonics in historical times: the example of the Bay of Aghios Andreas (Ilia, Greece). – *Z. Geomorph. N.F.* **42** (3): 367–372.
- FOUACHE, E. & DALONGEVILLE, R. (2004): Neotectonic impact on relative sea-level fluctuations over the past 6000 years: examples from Croatia, Greece and Southern Turkey. – CIESM (Commission Internationale pour l'Exploration Scientifique de la mer Méditerranée) Workshop Monographs **24**: 43–50; Monaco.
- FOUNTOULIS, I. (1994): Neotectonic evolution of Central-western Peloponnese, Greece. PhD Thesis, University of Athens, Faculty of Geology, Department of Dynamic Tectonic Applied Geology. – *Gaia* **7**: 386 pp.
- FÜCHTBAUER, H. (1988): *Sedimente und Sedimentgesteine*. – Ed. **4**: 1141 pp.; Schweizerbart, Stuttgart.
- FUJIWARA, O., MASUDA, F., SAKAI, T., IRIZUKI, T. & FUSE, K. (2000): Tsunami deposits in Holocene bay mud in southern Kanto region, Pacific coast of central Japan. – *Sediment. Geol.* **135**: 219–230.
- GAKI-PAPANASTASSIOU, K., MAROUKIAN, H., PAPANASTASSIOU, D., PALYVOS, N. & LEMEILLE, F. (2001): Geomorphological study in the Lokrian coast of northern Evoikos Gulf (central Greece) and evidence of palaeoseismic destructions. – *Rapports et Procès-verbaux des Réunions, Commission Internationale pour l'Exploration Scientifique de la Mer Méditerranée* **36**: 25.
- GELFENBAUM, G. & JAFFE, B. (2003): Erosion and Sedimentation from the 17 July, 1998 Papua New Guinea Tsunami. – *Pure Appl. Geophys.* **160**: 1969–1999.
- GEYH, M.A. (2005): *Handbuch der physikalischen und chemischen Altersbestimmung*. – 224 pp.; Wissenschaftliche Buchgesellschaft, Darmstadt.
- GIANFREDA, F., MASTRONUZZI, G. & SANSONO, P. (2001): Impact of historical tsunamis on a sandy coastal barrier: an example from the northern Gargano coast, southern Italy. – *Nat. Hazards and Earth Sys. Sci.* **1**: 213–219.
- GOFF, J., CHAGUÉ-GOFF, C. & NICHOL, S. (2001): Palaeotsunami deposits: a New Zealand perspective. – *Sediment. Geol.* **143**: 1–6.
- GROSKURD, C.G. (1831): *Strabo. Erdbeschreibung in siebzehn Büchern*. – Reprint of original edition, 1988, 4 volumes; Olms, Hildesheim.
- GUIDOBONI, E. & COMASTRI, A. (2005): Catalogue of earthquakes and tsunamis in the Mediterranean area from the 11<sup>th</sup> to the 15<sup>th</sup> century. – Vol. **2**: 1037 pp.; ING-SGA, Bologna.
- GUIDOBONI, E., COMASTRI, A. & TRAINA, G. (1994): Catalogue of ancient earthquakes in the Mediterranean area up to the 10<sup>th</sup> century. – Vol. **1**: 504 pp.; ING-SGA, Bologna.
- HAWKES, A.D., BIRD, M., COWIE, S., GRUNDY-WARR, C., HORTON, B.P., HWAI A.T.S., LAW, L., MACGREGOR, C., NOTT, J., ONG, J.E., RIGG, J., ROBINSON, R., TAN-MULLINS, M., SA, T.T., YASIN, Z. & AIK, L.W. (2007): Sediments deposited by the 2004 Indian Ocean Tsunami along the Malaysia-Thailand Peninsula. – *Marine Geol.* **242**: 169–190.
- HIEKE, W., HIRSCHLEBER, H.B. & DEHGHANI, G.A. (2003): The Ionian Abyssal Plain (central Mediterranean Sea): Morphology, subbottom structures and geodynamic history – an inventory. – *Marine geophys. Res.* **24**: 279–310; doi: 10.1007/s11001-004-2173-z.
- HINDSON, R.A. & ANDRADE, C. (1999): Sedimentation and hydrodynamic processes associated with the tsunami generated by the 1755 Lisbon earthquake. – *Quatern. Int.* **56**: 27–38.
- HINSBERGEN, D.J.J. VAN, LANGEREIS, C.G. & MEULENKAMP, J.E. (2005): Revision of the timing, magnitude and distribution of Neogene rotations in the western Aegean region. – *Tectonophysics* **396**: 1–34.

- HOLLENSTEIN, C., GEIGER, A., KAHLE, H.-G. & VEIS, G. (2006): CGPS time-series and trajectories of crustal motion along the West Hellenic Arc. – *Geophys. J. Int.* **164**: 182–191; doi: 10.1111/j.1365-246X.2005.02804.x.
- HOLLENSTEIN, C., MÜLLER, M.D., GEIGER, A. & KAHLE, H.-G. (2008a): Crustal motion and deformation in Greece from a decade of GPS measurements, 1993–2003. – *Tectonophysics* **449**: 17–40.
- HOLLENSTEIN, C., MÜLLER, M.D., GEIGER, A. & KAHLE, H.-G. (2008b): GPS-derived coseismic displacements associated with the 2001 Skyros and 2003 Lefkada earthquakes in Greece. – *Bull. Seismol. Soc. Amer.* **98** (1): 149–161.
- HUGHEN, K.A., BAILLIE, M.G.L., BARD, E., BAYLISS, A., BECK, J.W., BERTRAND, C.J.H., BLACKWELL, P.G., BUCK, C.E., BURR, G.S., CUTLER, K.B., DAMON, P.E., EDWARDS, R.L., FAIRBANKS, R.G., FRIEDRICH, M., GUILDERSON, T.P., KROMER, B., MCCORMAC, F.G., MANNING, S.W., BRONK RAMSEY, C., REIMER, P.J., REIMER, R.W., REMMELE, S., SOUTHON, J.R., STUIVER, M., TALAMO, S., TAYLOR, F.W., VAN DER PLICHT, J. & WEYHENMEYER, C.E. (2004): Marine04 Marine radiocarbon age calibration, 26 – 0 ka BP. – *Radiocarbon* **46**: 1059–1086.
- Institute of Geological and Mining research (IGMR) (1980): Geological map of Greece, 1:50,000, Pirgos Sheet; Athens.
- Institute of Geology and Mineral Exploration (IGME) (1985): Geological map of Greece, 1:50,000, Cephalonia Island (southern part); Athens.
- Institute of Geology and Mineral Exploration (IGME) (1996): Geological map of Greece, 1:50,000, Vonitsa Sheet; Athens.
- JING, Z. & RAPP, G. (2003): The coastal evolution of the Ambracian embayment and its relationship to archaeological settings. – In: WISEMAN, J. & ZACHOS, K. (eds.): *Landscape Archaeology in Southern Epirus, Greece I*. – Amer. School Class. Stud. Athens, Hesperia Suppl. **12**: 157–198.
- KAHLE, H.-G., MÜLLER, M. V., MUELLER, ST. & VEIS, G. (1993): The Kephallonia transform fault and the rotation of the Apulian Platform: evidence from satellite geodesy. – *Geophys. Res. Lett.* **20** (8): 651–654.
- KAHLE, H.-G., MÜLLER, M.V., GEIGER, A., DANUSER, G., MUELLER, ST., VEIS, G., BILLIRIS, H. & PARADISSIS, G. (1995): The strain field in NW Greece and the Ionian Islands: results inferred from GPS measurements. – *Tectonophysics* **249**: 41–52.
- KELLETAT, D. & SCHELLMANN, G. (2002): Tsunamis on Cyprus: Field evidences and <sup>14</sup>C dating results. – *Z. Geomorph. N.F., Suppl.* **137**: 19–34.
- KELLETAT, D. (1975): Untersuchungen zur Morphodynamik tropisch-subtropischer Küsten. Teil 4: Beobachtungen an holozänen Beachrock-Vorkommen des Peloponnes, Griechenland. – *Würzburger Geographische Arbeiten* **43**: 44–54.
- KELLETAT, D. (1998): Beachrock sensu stricto – Anmerkungen aus geomorphologischer Sicht. – *Kieler Geographische Schriften* **97**: 205–224.
- KELLETAT, D. (1999): *Physische Geographie der Meere und Küsten*. – 258 pp.; Teubner, Stuttgart, Leipzig.
- KELLETAT, D. (2005): Neue Beobachtungen zu Paläo-Tsunami im Mittelmeergebiet: Mallorca und Bucht von Alanya, türkische Südküste. – In: BECK, N. (ed.): *Neue Ergebnisse der Meeres- und Küstenforschung*. – *Schriften des Arbeitskreises Landes- und Volkskunde Koblenz (ALV)* **4**: 1–14.
- KELLETAT, D. (2006): Beachrock as sea-level indicator? Remarks from a geomorphological point of view. – *J. Coastal Res.* **22** (6): 1558–1564.
- KELLETAT, D. (2007): Reply to: KNIGHT, J. (2007): Beachrock reconsidered. – Discussion of: KELLETAT, D. (2006): Beachrock as sea-level indicator? Remarks from a geomorphological point of view; *J. Coastal Res.* **22** (6): 1558–1564. – *J. Coastal Res.* **23** (6): 1605–1606.

- KELLETAT, D., KOWALCZYK, G., SCHRÖDER, B. & WINTER, K.P. (1976): A synoptic view on the neotectonic development of Peloponnesian coastal regions. – *Z. dt. Geol. Gesell.* **127**: 447–465.
- KNIGHT, J. (2007): Beachrock reconsidered. Discussion of: KELLETAT, D. (2006): Beachrock as sea-level indicator? Remarks from a geomorphological point of view; *J. Coastal Res.* **22** (6): 1558–1564. – *J. Coastal Res.* **23** (4): 1074–1078.
- KONTOPOULOS, N. & AVRAMIDIS, P. (2003): A late Holocene record of environmental changes from the Aliko lagoon, Egion, North Peloponnesus, Greece. – *Quatern. Int.* **111**: 75–90.
- KORTEKAAS, S. (2002): Tsunamis, storms and earthquakes: Distinguishing coastal flooding events. – PhD Thesis, Univ. Coventry; Coventry, Great Britain.
- KORTEKAAS, S. & DAWSON, A.G. (2007): Distinguishing tsunami and storm deposits: An example from Martinhal, SW Portugal. – *Sediment. Geol.* **200**: 208–221.
- KOWALCZYK, G. & WINTER, P.K. (1979): Die geologische Entwicklung der Kyllini-Halbinsel im Neogen und Quartär. – *Z. dt. Geol. Gesell.* **130**: 323–346.
- KRAFT, J.C. & RAPP, G. (RIP), GIFFORD, J.A. & ASCHENBRENNER, S.E. (2005): Coastal change and archaeological settings in Elis. – *Amer. School Class. Stud. Athens, Hesperia* **74** (1): 1–39.
- LAGIOS, E., SAKKAS, V., PAPADIMITRIOU, P., PARCHARIDIS, I., DAMIATA, B.N., CHOUSIANITIS, K. & VASSILOPOULOU, S. (2007): Crustal deformation in the Central Ionian Islands (Greece): Results from DGPS and DInSAR analyses (1995–2006). – *Tectonophysics* **444**: 119–145.
- LEKKAS, E., FOUNTOULIS, I. & PAPANIKOLAOU, D. (2000): Intensity distribution and neotectonic macrostructure Pyrgos earthquake data (26 March 1993, Greece). – *Nat. Hazards* **21**: 19–33.
- LIENAU, C. (1989): Griechenland. Geographie eines Staates der europäischen Südperipherie. – *Wissenschaftliche Länderkunden* **32**; Darmstadt.
- MAOUCHE, S., MORHANGE, C. & MEGHRAOUI, M. (2009): Large boulder accumulation on the Algerian coast evidence tsunami events in the western Mediterranean. – *Marine Geol.* **262**: 96–104.
- MARIOLAKOS, I., LEKKAS, E., DANAMOS, G., LOGOS, E., FOUNTOULIS, I. & ADAMOPOULOU, E. (1991): Neotectonic evolution of the Kyllini Peninsula (N.W. Peloponnesus). – *Bull. Geol. Soc. Greece* **25** (3): 163–176.
- MAROUKIAN, H., GAKI-PAPANASTASSIOU, K., PAPANASTASSIOU, D. & PALYVOS, N. (2000): Geomorphological observations in the coastal zone of Kyllini peninsula, NW Peloponnesus-Greece, and their relation to the seismotectonic regime of the area. – *J. Coast. Res.* **16** (3): 853–863.
- MASTRONUZZI, G. & SANSÒ, P. (2000): Boulder transport by catastrophic waves along the Ionian coast of Apulia (southern Italy). – *Marine Geol.* **170** (1–2): 93–103.
- MASTRONUZZI, G. & SANSÒ, P. (2004): Large boulder accumulations by extreme waves along the Adriatic coast of southern Apulia (Italy). – *Quatern. Int.* **120**: 173–184.
- MASTRONUZZI, G., PIGNATELLI, C., SANSÒ, P. & SELLERI, G. (2007): Boulder accumulations produced by the 20th of February, 1743 tsunami along the coast of southeastern Salento (Apulia region, Italy). – *Marine Geol.* **242**: 191–205.
- MAY, S.M., VÖTT, A., BRÜCKNER, H. & BROCKMÜLLER, S. (2007): Evidence of tsunamigenic impact on Actio headland near Preveza, NW Greece. – In: GÖNNERT, G., PFLÜGER, B. & BREMER, J.-A. (eds.): *Von der Geoarchäologie über die Küstendynamik zum Küstenzonenmanagement*. – *Coastline Rep.* **9**: 115–125.
- MAY, S.M., WILLERSHÄUSER, T. & VÖTT, A. (2009): Boulder transport by high-energy wave events at Cape Bon (NE Tunisia). – *Coastline Rep.* (in press).
- MCCCLUSKY, S., BALASSANIAN, S., BARKA, A., DEMIR, C., ERGINTAV, S., GEORGIEV, I., GURKAN, O., HAMBURGER, M., HURST, K., KAHLE, H., KASTENS, K., KEKELIDZE, G., KING, R., KOTZEV, V., LENK, O., MAHMOUD, S., MISHIN, A., NADARIYA, M., OUZOUNIS, A., PARADISSIS, D., PETER, Y., PRILEPIN, M., REILINGER, R., SANLI, I., SEEGER, H., TEALEB, A., TOKSOZ, M. N. & VEIS, G. (2000): Global Positioning System constraints on plate kinematics and dynamics in the eastern Mediterranean and Caucasus. – *J. Geophys. Res., Solid Earth* **105** (3): 5695–5719.

- McCoy, F.W. & Heiken, G. (2000): Tsunami generated by the Late Bronze Age eruption of Thera (Santorini), Greece. – *Pure Appl. Geophys.* **157**: 1227–1256.
- Moore, A., Nishimura, Y., Gelfenbaum, G., Kamataki, T. & Triyono, R. (2006): Sedimentary deposits of the 26 December 2004 tsunami on the northwest coast of Aceh, Indonesia. – *Earth Planets Space* **58**: 253–258.
- MORHANGE, C., MARRINER, N. & PIRAZZOLI, P.A. (2006a): Evidence of late-Holocene tsunami events in Lebanon. – In: SCHEFFERS, A. & KELLETAT, D. (eds.): *Tsunamis, hurricanes and neotectonics as driving mechanisms in coastal evolution*. – *Z. Geomorph. N.F. Suppl.* **146**: 81–95.
- MORHANGE, C., PIRAZZOLI, P.A., MARRINER, N., MONTAGGIONI, L.F. & NAMMOUR, T. (2006b): Late Holocene relative sea-level changes in Lebanon, Eastern Mediterranean. – *Marine Geol.* **230**: 99–114.
- MORTON, R.A., GELFENBAUM, G. & JAFFE, B.E. (2007): Physical criteria for distinguishing sandy tsunami and storm deposits using modern examples. – *Sediment. Geol.* **200**: 184–207.
- MURRAY, A.S. & WINTLE, A.G. (2000): Luminescence dating of quartz using an improved single-aliquot regenerative-dose protocol. – *Radiation Measurements* **32** (1): 57–73.
- National Geophysical Data Center (NGDC, 2009): NOAA/WDC Historical Tsunami Database at NGDC. – [http://www.ngdc.noaa.gov/hazard/tsu\\_db.shtml](http://www.ngdc.noaa.gov/hazard/tsu_db.shtml) (access: 2009/03/15).
- NISHIMURA, Y. & MIYAJI, N. (1995): Tsunami deposits from the 1993 southwest Hokkaido earthquake and the 1640 Hokkaido Komagatake Eruption, northern Japan. – *Pageoph* **144** (3–4): 719–733.
- PANTOSTI, D., BARBANO, M.S., SMEDILE, A. & DE MARTINI, P.M. (2008): Geological evidence of palaeotsunamis at Torre degli Inglesi (northeast Sicily). – *Geophys. Res. Lett.* **35**: L05311; doi: 10.1029/2007GL032935.
- PAPADOPOULOS, G.A. (2001): Tsunamis in the east Mediterranean: a catalogue for the area of Greece and adjacent seas. – *Proceedings Joint IOC-IUGG International Workshop Tsunami Risk Assessment Beyond 2000: Theory, Practice and Plans*, June 14–16, 2000. – 34–43; Moscow (vgl.: National Observatory of Athens (NOA, 2001)).
- PAPADOPOULOS, G.A. & FOKAEFS, A. (2005): Strong tsunamis in the Mediterranean Sea: a re-evaluation. – *ISET J. Earthquake Technol.* **42** (4): 159–170, paper 463.
- PAPADOPOULOS, G.A., DASKALAKI, E., FOKAEFS, A. & GIRALEAS, N. (2007): Tsunami hazards in the eastern Mediterranean: strong earthquakes and tsunamis in the East Hellenic Arc and Trench system. – *Nat. Hazards and Earth Sys. Sci.* **7**: 57–64.
- PAPAZACHOS, B.C. & DIMITRIU, P.P. (1991): Tsunamis in and near Greece and their relation to the earthquake focal mechanism. – In: BERNARD, E.N. (ed.): *Tsunami hazard. A practical guide for tsunami hazard reduction*. – *Nat. Hazards* **4** (2–3): 161–170.
- PAPAZACHOS, B.C. & KIRATZI, A.A. (1996): A detailed study of the active crustal deformation in the Aegean and surrounding area. – *Tectonophysics* **253**: 129–153.
- PAPAZACHOS, B.C. & PAPAACHOU, C. (1997): *The earthquakes of Greece*. – 304 pp.; Ziti, Thessaloniki.
- PARIS, R., LAVIGNE, F., WASSMER, P. & SARTOHADI, J. (2007): Coastal sedimentation associated with the December 26, 2004 tsunami in Lhok Nga, west Banda Aceh (Sumatra, Indonesia). – *Marine Geol.* **238**: 93–106.
- PETER, Y. (2001): Present-day crustal dynamics in the Adriatic-Aegean plate boundary zone inferred from continuous GPS-measurements. – *ETH Zürich, Institut für Geodäsie und Photogrammetrie Mitteilungen* **71**.
- PIRAZZOLI, P.A., STIROS, S.C., ARNOLD, M., LABOREL, J., LABOREL-DEGUEN, F. & PAPAGEORGIOU, S. (1994): Episodic uplift deduced from Holocene shorelines in the Perachora Peninsula, Corinth area, Greece. – *Tectonophysics* **229** (3–4): 201–209.
- PIRAZZOLI, P.A., STIROS, S.C., ARNOLD, M., LABOREL, J. & LABOREL-GEUEN, F. (1999): Late Holocene coseismic vertical displacement and tsunami deposits near Kynos, Gulf of Euboea, central Greece. – *Physics and Chemistry of the Earth (A)* **24** (4): 361–367.

- RAPHAEL, C.N. (1973): Late Quaternary changes in coastal Elis, Greece. – *Geograph. Rev.* **63**: 73–89.
- RAPHAEL, C.N. (1978): The Erosional History of the Plain of Elis in the Peloponnese. – In: BRICE, W.C. (ed.): *The environmental history of the Near and Middle East since the last ice age.* – 51–66; London, New York, San Francisco.
- REIMER, P.J. & McCORMAC, F.G. (2002): Marine radiocarbon reservoir corrections for the Mediterranean and Aegean Seas. – *Radiocarbon* **44**: 159–166.
- REIMER, P.J., BAILLIE, M.G.L., BARD, E., BAYLISS, A., BECK, J.W., BERTRAND, C.J.H., BLACKWELL, P.G., BUCK, C.E., BURR, G.S., CUTLER, K.B., DAMON, P.E., EDWARDS, R.L., FAIRBANKS, R.G., FRIEDRICH, M., GUILDERTON, T.P., HOGG, A.G., HUGHEN, K.A., KROMER, B., McCORMAC, F.G., MANNING, S.W., RAMSEY, C.B., REIMER, R.W., REMMELE, S., SOUTHON, J.R., STUIVER, M., TALAMO, S., TAYLOR, F.W., VAN DER PLICHT, J. & WEYHENMEYER, C.E. (2004): IntCal04 Terrestrial radiocarbon age calibration, 26 – 0 ka BP. – *Radiocarbon* **46**: 1029–1058.
- REIMER, P.J., BAILLIE, M.G.L., McCORMAC, G., REIMER, R.W., BARD, E., BECK, J.W., BLACKWELL, P.G., BUCH, C.E., BURR, G.S., EDWARDS, R.L., FRIEDRICH, M., GUILDERTON, T.P., HOGG, A.G., HUGHEN, K.A., KROMER, B., MANNING, S., SOUTHON, J.R., VAN DER PLICHT, J. & WEYHENMEYER, C.E. (2006): Comment on “Radiocarbon calibration curve spanning 0 to 50,000 years BP based on paired  $^{230}\text{Th}/^{234}\text{U}/^{238}\text{U}$  and  $^{14}\text{C}$  dates on pristine corals” by R.G. FAIRBANKS et al. (*Quaternary Science Reviews* **24** (2005) 1781–1796) and “Extending the radiocarbon calibration beyond 26,000 years before present using fossil corals” by T.-C. CHIU et al. (*Quaternary Science Reviews* **24** (2005) 1797–1808). – *Quatern. Sci. Rev.* **25**: 855–862.
- REINHARDT, E.G., GOODMAN, B.N., BOYCE, J.I., LOPEZ, G., VAN HENSTUM, P., RINK, W.J., MART, Y. & RABAN, A. (2006): The tsunamis of 13 December A.D. 115 and the destruction of Herod the Great’s harbor at Caesarea Maritima, Israel. – *Geology* **34** (12): 1061–1064.
- RICHMOND, B., JAFFE, B.E., GELFENBAUM, G. & MORTON, R.A. (2006): Geologic impacts of the 2004 Indian Ocean tsunami on Indonesia, Sri Lanka, and the Maldives. – *Z. Geomorph. N.F. Suppl.* **146**: 235–251.
- SACHPAZI, M., HIRN, A., CLÉMENT, C., HASLINGER, F., LAIGLE, M., KISSLING, E., CHARVIS, P., HELLO, Y., LÉPINE, J.-C., SAPIN, M. & ANSORGE, J. (2000): Western Hellenic subduction and Cephalonia Transform: local earthquakes and plate transport and strain. – *Tectonophysics* **319** (4): 301–319.
- SATO, H., SHIMAMOTO, T., TSUTSUMI, A. & KAWAMOTO, E. (1995): Onshore tsunami deposits caused by the 1993 southwest Hokkaido and 1983 Japan Sea Earthquakes. – *Pageoph* **144** (3–4): 693–710.
- SCHAEFFER, F. & SCHACHTSCHABEL, P. (2002): *Lehrbuch der Bodenkunde.* – Ed. **15**: 593 pp.; Spektrum Akademischer Verlag, Heidelberg, Berlin.
- SCHAEFFERS, A. & SCHAEFFERS, S. (2007): Tsunami deposits on the coastline of west Crete (Greece). – *Earth and Planet. Sci. Lett.* **259** (3–4): 613–624.
- SCHAEFFERS, A., KELLETAT, D., VÖTT, A., MAY, S.M. & SCHAEFFERS, S. (2008): Late Holocene tsunami traces on the western and southern coastlines of the Peloponnese (Greece). – *Earth Planet. Sci. Lett.* **269**: 271–279.
- SCHIELEIN, P., ZSCHAU, J., WOITH, H. & SCHELLMANN, G. (2007): Tsunamigefährdung im Mittelmeer – Eine Analyse geomorphologischer und historischer Zeugnisse. – *Bamberger Geographische Schriften* **22**: 153–199.
- SCICCHITANO, G., MONACO, C. & TORTORICI, L. (2007): Large boulder deposits by tsunami waves along the Ionian coast of south-eastern Sicily (Italy). – *Marine Geol.* **238**: 75–91.
- SHAW, B., AMBRAYSES, N.N., ENGLAND, P.C., FLOYD, M.A., GORMAN, G.J., HIGHHAM, T.F.G., JACKSON, J.A., NOCQUET, J.-M., PAIN, C.C. & PIGGOTT, M.D. (2008): Eastern Mediterranean tectonics and tsunami hazard inferred from the AD 365 earthquake. – *Nat. Geosci.*; <http://www.nature.com/doi/10.1038/ngeo151>.

- SHI, S., DAWSON, A. & SMITH, D.E. (1995): Coastal sedimentation associated with the December 12<sup>th</sup>, 1992 tsunami in Flores, Indonesia. – *Pageoph* **144** (3–4): 525–536.
- SHORT, A.D. (2005): Carbonate sandy beaches. – In: SCHWARTZ, M.L. (ed.): *Encyclopedia of coastal science*. – 218–221; Dordrecht.
- SOLOVIEV, S.L., SOLOVIEVA, O.N., GO, C.N., KIM, K.S. & SHCHETNIKOV, N.A. (2000): Tsunamis in the Mediterranean Sea 2000 B.C.–2000 A.D. – 237 pp.; Kluwer, Dordrecht.
- STAMATOPOULOS, L., VOLTAGGIO, M., KONTOPOULOS, N., CINQUE, A. & LA ROCCA, S. (1988): <sup>230</sup>Th/<sup>238</sup>U dating of corals from Thyrrhenian marine deposits of Varda area (north-western Peloponnesus), Greece. – *Geogr. Fis. e Dinam. del Quatern.* **11**: 99–103.
- STAMATOPOULOS, L., VOLTAGGIO, M. & KONTOPOULOS, N. (1994): <sup>230</sup>T/<sup>238</sup>U-Dating of corals from Tyrrhenian marine deposits and the Paleogeographic Evolution of the Western Peloponnesus (Greece). – *Münstersche Forschungen zur Geologie und Paläontologie* **76**: 345–352.
- STANLEY, J.-D. & BERNASCONI, M.P. (2006): Holocene depositional patterns and evolution in Alexandria's eastern harbor, Egypt. – *J. Coastal Res.* **22** (2): 283–297.
- STIROS, S. C., ARNOLD, M., PIRAZZOLI, P. A., LABOREL, J. & LABOREL-DEGUEN, F. (1994): The 1953 earthquake in Cephalonia (western Hellenic arc): Coastal uplift and halotectonic faulting. – *Geophys. J. Int.* **117**: 834–849.
- TINTI, S., MARAMAI, A. & GRAZIANI, L. (2004): The new catalogue of Italian tsunamis. – *Nat. Hazards* **33** (3): 439–465.
- TURNER, R.J. (2005): Beachrock. – In: SCHWARTZ, M.L. (ed.): *Encyclopedia of coastal science*. – 24–25; Dordrecht.
- UNDERHILL, J. (1988): Triassic evaporites and Plio-Quaternary diapirism in western Greece. – *J. Geol. Soc.* **145**: 269–282; London.
- UNDERHILL, J.R. (1989): Late Cenozoic deformation of the Hellenide foreland, western Greece. – *Geol. Soc. Amer. Bull.* **101**: 613–634.
- VÖTT, A. (2007): Relative sea level changes and regional tectonic evolution of seven coastal areas in NW Greece since the mid-Holocene. – *Quatern. Sci. Rev.* **26**: 894–919.
- VÖTT, A., MAY, M., BRÜCKNER, H. & BROCKMÜLLER, S. (2006): Sedimentary evidence of late Holocene tsunami events near Lefkada Island (NW Greece). – In: SCHEFFERS, A. & KELLETAT, D. (eds.): *Tsunamis, hurricanes and neotectonics as driving mechanisms in coastal evolution*. – *Z. Geomorph. N.F. Suppl.* **146**: 139–172.
- VÖTT, A., BRÜCKNER, H., MAY, M., LANG, F. & BROCKMÜLLER, S. (2007): Late Holocene tsunami imprint on Actio headland at the entrance to the Ambrakian Gulf. – *Méditerranée* **108**: 43–57.
- VÖTT, A., BRÜCKNER, H., MAY, M., LANG, F., HERD, R. & BROCKMÜLLER, S. (2008): Strong tsunami impact on the Bay of Aghios Nikolaos and its environs (NW Greece) during Classical-Hellenistic times. – *Quatern. Int.* **181**: 105–122.
- VÖTT, A., BRÜCKNER, H., BROCKMÜLLER, S., HANDL, M., MAY, S.M., GAKI-PAPANASTASSIOU, K., HERD, R., LANG, F., MAROUKIAN, H., NELLE, O. & PAPANASTASSIOU, D. (2009a): Traces of Holocene tsunamis across the Sound of Lefkada, NW Greece. – *Global and Planetary Change* **66**: 112–128; Amsterdam.
- VÖTT, A., BRÜCKNER, H., MAY, S.M., SAKELLARIOU, D., NELLE, O., LANG, F., KAPSIMALIS, V., JAHNS, S., HERD, R., HANDL, M. & FOUNTOULIS, I. (2009b): The Lake Voulkaria (Akarnania, NW Greece) palaeoenvironmental archive – a sediment trap for multiple tsunami impact since the mid-Holocene. – *Z. Geomorph. N.F. Suppl.* **53** (1): 1–37.
- VOUSDOKAS, M.I., VELEGRAKIS, A.F. & PLOMARITIS, T.A. (2007): Beachrock occurrence, characteristics, formations mechanisms and impacts. – *Earth-Sci. Rev.* **85**: 23–46.
- YALOURIS, N. (1957): Δοκιμαστικά έρευναί εις τόν κόλπρον τής Φειάς Ηλείας. – *ArchEph* **1957**: 31–43.
- YALOURIS, N. (1960): Φειά. – *ArchDelt* **16 B**: 126.

YIM, W.W.-S., IVANOVICH, M. & YU, K.-F. (1990): Younger age bias of radiocarbon dates in pre-Holocene marine deposits of Hong Kong and implications for Pleistocene Stratigraphy. – *Geo-Marine Lett.* **10**: 165–172.

Addresses of the authors:

A. Vött, G. Bareth, H. Brückner, C. Curdt, H. Hadler, D. Hoffmeister, N. Klasen, S.M. May, K. Ntageretzi and T. Willershäuser, Institute for Geography, Universität zu Köln, Albertus-Magnus-Platz, 50923 Köln (Cologne), Germany

I. Fountoulis, Department of Dynamic, Tectonic, Applied Geology, National and Kapodistrian University of Athens, Panepistimiopolis, 15784 Athens, Greece

R. Grapmayer, In der Ecke 1, Grünberg-Stangenrod, 35305 Grünberg, Germany

F. Lang, Department of Classical Archaeology, Technische Universität Darmstadt, El-Lissitzky-Str. 1, 64287 Darmstadt, Germany

P. Masberg, Mineralogical Museum, Philipps-Universität Marburg, Firmanenplatz, 35032 Marburg/Lahn, Germany

D. Sakellariou, Hellenic Centre for Marine Research, 19013 Anavissos, Greece.

\*Corresponding author: andreas.voett@uni-koeln.de